Chemically Modified Oligonucleotides Silence Mutant SPTLC1 in an in vitro Model of HSAN1

CHEMICALLY MODIFIED OLIGONUCLEOTIDES SILENCE MUTANT SPTLC1 IN AN IN VITRO MODEL OF HSAN1

A Masters Thesis Presented

By

HAVISHA BINDU KARNAM

Submitted to the Faculty of the

University of Massachusetts Graduate School of Biomedical Sciences, Worcester

in partial fulfillment of the requirements for the degree of

MASTER OF SCIENCE

September 5th, 2018

BIOMEDICAL SCIENCES

CHEMICALLY MODIFIED OLIGONUCLEOTIDES SILENCE MUTANT SPTLC1 IN AN IN VITRO MODEL OF HSAN1

A Masters Thesis Presented

By

HAVISHA BINDU KARNAM

The signatures of the Master's Thesis Committee signify completion and approval as to style and content of the Thesis

David Weaver, Ph.D., Chair of Committee

Jonathan Watts, Ph.D., Member of Committee

Mary Ellen Lane, Ph.D., Member of Committee

The signature of the Dean of the Graduate School of Biomedical Sciences signifies that the student has met all master's degree graduation requirements of the school.

Mary Ellen Lane, Ph.D.,

Dean of the Graduate School of Biomedical Sciences

Biomedical Sciences

September 5th, 2018

Acknowledgements

I would like to thank Dr. Brown and Dr. Khvorova for providing me the opportunity to work and interact with world-class scientists at UMass and the chance to use cutting-edge technology on a project that may one day impact patients' lives for the better. Thanks especially to Dr. Brown for funding this work and to both for overseeing it and providing feedback.

Thanks to all those who taught me and helped me perform experiments. A sincere thanks to Dr. Andrew Coles and various Khvorova lab members for help in preparing mouse primary cortical neurons. Thank you to Dimas Echevarria and Matthew Hassler for making oligonucleotides for my project. Thank you to Julia Alterman for teaching me how to perform the branched DNA assay. I really appreciated Nick Wightman for his help in learning western blots and for his technical advice whenever I asked. Thanks so much to Jake Metterville for helping me with mouse work as well as intrathecal injections, as well as Alex Weiss for teaching me about animal husbandry. A special thanks to Courtney Pinto for her hard work maintaining the HSAN1 mouse colony and for setting up timed pregnancies.

Importantly, I would like to thank my loving and supportive family and close friends and program-mates, who have stood by me and cared for me no matter what.

Abstract

Hereditary sensory and autonomic neuropathy type 1 (HSAN1) is a monogenic, autosomal dominantly inherited, neurodegenerative disorder resulting in loss of pain and temperature sensation in the distal limbs. HSAN1 is caused by point mutations in a single allele of serine palmitoyltransferase long chain base 1 (SPTLC1), resulting in production of neurotoxic deoxysphingolipids (dSLs). Oligonucleotide therapeutics (ONTs) can be used to downregulate the mutant allele and/or the wild type allele and thus are viable treatment strategies. We investigated the ability of two classes of ONTs, short interfering RNAs (siRNAs) and antisense oligonucleotides (ASOs), to downregulate SPTLC1 in an in vitro model of HSAN1 derived from the C133W mouse model overexpressing mutant *hamster* SPTLC1. We screened a panel of siRNAs and ASOs targeting mutant *hamster* SPTLC1 and identified four lead compounds. We demonstrated these compounds' ability to reduce mutant *hamster* SPLTC1 and/or wild type *mouse* SPTLC1 mRNA in CHO cells and C57BL/6J embryonic mouse primary cortical neurons. We then showed that these compounds downregulate *hamster* and *mouse* SPTLC1 mRNA and protein in embryonic primary cortical neuron cultures derived from C133W mice. These compounds demonstrate therapeutic potential and should be developed further in vivo.

Table of Contents

List of Tables

List of Figures

List of Third Party Copyrighted Material

Preface

This thesis constitutes the written culmination of work done in fulfillment of the Master of Science degree at the University of Massachusetts Medical School Graduate School of Biomedical Sciences. The work done was supported by Dr. Robert H. Brown, Jr. Chair of the Department of Neurology, and was conducted under the supervision of both Dr. Brown and Dr. Anastasia Khvorova in the RNA Therapeutics Institute. All figures with the exception of Appendix Figure 2 and all data in this document were generated by me, with the input of Dr. Khvorova and Dr. Brown. Appendix Figure 2. Dorsal Root Ganglion cellular structure was published by Karen Hart of Peninsula College, who has given permission for reproduction of this figure in this document.

Introduction

Hereditary sensory and autonomic neuropathy Type 1 (HSAN1) is an autosomal dominantly inherited, neurodegenerative disorder with onset in early adulthood (McCampbell, Truong et al. 2005). It is characterized initially by painful hypersensitivity to minimal stimuli, which progresses to loss of pain and temperature sensation primarily affecting distal limbs (Auer-Grumbach 2008),(Nicholson 2006). The underlying pathology, which correlates well with symptomatology, entails loss of small myelinated and unmyelinated sensory nerve fibers and their corresponding dorsal root ganglia (Garofalo, Penno et al. 2011). Denervation of distal limb muscles leads to wasting and weakness in some cases (McCampbell, Truong et al. 2005). In some individuals there is compromise of autonomic nerve function as well, although this is not a prominent aspect of HSAN1 (Eichler 2018).

The first description of the molecular basis of HSAN1 followed genetic linkage analysis in large HSAN1 families in Australia (Nicholson, Dawkins et al. 2001) and identification of missense mutations in the gene serine palmitoyltransferase long chain base 1 (SPTLC1) (Dawkins, Hulme et al. 2001), encoding the protein long chain base 1 (LCB1). LCB1 is a subunit of enzyme serine palmitoyltransferase (SPT) (Bejaoui, Wu et al. 2001). To date, several disease-associated point mutations in the *SPTLC1* gene have been identified, including C133W, C133Y, V144D, C133R, A352V, S331F, and S331Y (Garofalo, Penno et al. 2011), (Bode, Bourquin et al. 2016), (Suh, Hong et al. 2014).

SPT normally catalyzes the condensation of serine with palmitoyl coA to form 3-keto-sphinganine; this is the initial, rate-limiting step of ceramide and sphingolipid biosynthesis (Hanada 2003). The disease-causing mutations cluster around the active site of SPT and perturb the geometry of the active site (Eichler, Hornemann et al. 2009), rendering it more promiscuous and permitting alanine and glycine as well as serine to react with palmitoyl coA (Penno, Reilly et al. 2010). This reaction produces two neurotoxic deoxysphingolipids (dSLs), 1-deoxysphinganine (doxSA) and 1-deoxymethylsphinganine (doxSO), that are thought to be causative agents of disease (Penno, Reilly et al. 2010). Thus the disease-causing mutations represent a toxic gain of function.

We believe modulation of SPTLC1 is a potential treatment strategy for HSAN1, with allele-specific reduction being the optimal strategy. Previous studies show that the ratio of wild type to mutant SPTLC1 impacts disease severity in the C133W mouse model while homozygous knockout mice exhibit embryonic lethality (Eichler, Hornemann et al. 2009). Allele-specific silencing would enable downregulation of the toxic allele while preserving function of the wild type allele. Several lines of evidence establish that dSL levels influence disease severity (Garofalo, Penno et al. 2011). So, even reduction of both wild type and mutant SPTLC1 may also be beneficial. This strategy necessitates that the degree of silencing of both alleles is high enough to reduce toxic dSLs to below the disease-causing threshold but not enough to cause problems due to lack of gene expression. McCampbell et al. previously developed a mouse model overexpressing

mutant hamster C133W in a wild type mouse background and accurately recapitulating the HSAN1 disease phenotype, including the production of toxic dSLs (McCampbell, Truong et al. 2005). Downregulating SPTLC1 in the C133W model uniquely allows investigation of the biological consequences of SPTLC1 modulation by enabling differential targeting of mutant and wild type SPTLC1 on the basis of gene sequence differences in hamster (mutant) SPTLC1 and mouse (wild type) SPTLC1.

The antisense oligonucleotide (ASO) and short interfering RNA (siRNA) classes of oligonucleotide therapeutics have had several recent successes in clinical development. Double stranded siRNA therapeutic patisiran, designed by Alnylam to treat hATTR (hereditary amyloidogenic transthyretin) Amyloidosis, completed a Phase III trial with a promising efficacy and side effect profile (2018). The FDA also recently approved the first Gapmer ASO drug, mipomersen, for homozygous familial hypercholesterolemia (Shen and Corey 2017). Gapmers are single-stranded ASOs with a central DNA "gap," flanked by chemically modified nucleotides (Khvorova and Watts 2017). ASOs and siRNAs have also been shown to be effective in the treatment of central nervous system conditions. For example, nusinersen is a splice-switching ASO that is the first FDA-approved drug for treatment of Spinal Muscular Atrophy (Shen and Corey 2017). Splice-switching ASOs are oligonucleotides that bind to pre-mRNAs and disrupt normal splicing, leading to an altered set of spliced transcripts (Watts and Corey 2012). This is in contrast to Gapmer ASOs, which function by forming a heteroduplex of DNA and RNA by base pairing with the target mRNA and recruiting RNase H to cleave the target

(Khvorova and Watts 2017). The Khvorova lab also previously showed that chemically modified siRNAs can ameliorate the Huntington phenotype in a mouse model (Alterman, Hall et al. 2015).

Thus, we set out to conduct a proof of concept study investigating the impact of ASOs and chemically modified siRNAs downregulating hamster SPTLC1 in an in vitro context. We designed, synthesized, and screened a panel of siRNAs and chemically modified ASOs and identified compounds that target hamster SPTLC1. We also identified a compound solely targeting mouse SPTLC1. We showed that these compounds demonstrate efficacy in Chinese hamster ovary (CHO-K1) cells, mouse cortical primary neurons, or both. We then utilized an in vitro model for assessing knockdown of SPTLC1 by deriving primary embryonic cortical neurons from C133W transgenic mice and demonstrated reduction in the appropriate mRNA and protein. We also evaluated the impact of these compounds on dSL levels in this system. Thus this study describes the development and validation of novel ASOs and chemically stabilized siRNAs which allow modulation of hamster SPTLC1. These compounds can be used to evaluate the feasibility of oligonucleotide therapeutics for treatment of HSAN1 in the future.

Materials and Methods

Oligonucleotide Synthesis, Deprotection, and Purification

Oligonucleotide synthesis, deprotection, and purification were conducted as described previously (Osborn, Coles et al. 2018). Oligonucleotides were synthesized on an Expedite Applied Biosystems DNA/RNA Synthesizer following standard protocols. Each synthesis was done on a 1 µmole scale using cholesterol-conjugated controlled pore glass (CPG) solid supports for the sense strand and Unylinker solid support (ChemGenes, USA) for the antisense strand.

Cell culture

CHO-K1 cells (ATCC, USA) were grown in F12-K medium (ATCC, USA) supplemented with 10% fetal bovine serum (FBS; Gibco, USA) and 1% penicillin/streptomycin (Invitrogen, USA). Cells were maintained at 37 °C with 5% CO_2, and were subcultured 1:4-1:8 every 2-3 days with medium renewal once between subcultures. Cultures were discarded after 15 passages.

Preparation of primary neurons

Primary neuron cultures were prepared using a previously described method (Alterman, Coles et al. 2017). Briefly, pregnant females were euthanized by isoflurane overdose and uterine horns were dissected out and placed into a petri dish containing DMEM. Individual embryos were removed from the uterus and brains of individual embryos were dissected out and placed into a petri dish containing Hibernate E (Thermo Fisher, USA).

Cortices were microdissected out and chemically dissociated for 30 minutes using a pre-warmed solution of DNAse I (Worthington, USA) and papain (Worthington, USA). The dissociation solution was then removed and cortices were resuspended in complete NeuralQ medium (Sigma Aldrich, USA) supplemented with 2.5% FBS and mechanically disrupted by passing them repeatedly through a glass-blown Pasteur pipette. Cortical neurons were counted and plated at 1×10^5 cells per ml in precoated poly-L-lysine 96 well-plates. (BD BIOCOAT, Corning, USA).

For transgenic primary cortical neuron cultures, heterozygous transgenic C133W mice (C57BL/6J) were crossed with wild type C57BL/6J mice to produce a heterogeneous pool of heterozygous transgenic mice and wild type mice. All embryos from each litter were used to generate homogenous transgenic cultures, which were pooled and then aliquoted. Thus, the different wells in each experiment should theoretically contain the same ratio of transgene/WT SPTLC1. Primary cortical neurons were harvested from FVB/NJ mouse embryos for wild type mouse cultures or embryos from crossing transgenic and wild type mice for transgenic cultures at embryonic day 15.5-17.5.

Genotyping

Several C133W transgenic lines were developed previously. Here, animals from the 8E line were used. Animals were genotyped as follows: tail snips were taken at ~28 days of age and tissue was processed using the DNeasy blood and tissue extraction kit. The transgene was detected by multiplex PCR amplification DNA using the following primers: F, 5′-CGAAAAACCATCCTGCTCTC-3′; R, 5′-

GGACAGACGGTTCCAGTGTT-3′ for the transgene, and F, 5′-GAGGGAGGTGGAAGGAAAGA-3′; R. 5′-GAAGGGTTGTTGCTCTGACC-3′ for the mouse ABCD1 gene, a positive control.

Lipid-mediated delivery of oligonucleotides in cell lines

For LNA (Locked Nucleic Acid) Gapmer screen experiments assaying knockdown of mRNA, CHO-K1 cells were plated in cell solution (CHO-K1 cells in F12-K medium supplemented with 6% FBS) at a density of 10,000 cells per well in 96-well tissue culture plates. OptiMEM was used to dilute compounds to 400 nM concentration. RNAiMax (Thermo Fisher, USA) was diluted to 1.2% concentration and an equal volume of the solution was added to the compounds. Cells were treated by adding 50 µl of diluted hsiRNA to 50 µl of cell solution, resulting in a final FBS concentration of 3% and final compound concentration of 100nM. Cells were incubated for 72 hours before harvesting for mRNA quantification.

Passive delivery of oligonucleotides in cell lines

For mRNA dose response experiments in CHO-K1 cells, CHO-K1 cells were plated in F12-K medium supplemented with 6% FBS at a density of 10,000 cells per well in 96-well tissue culture plates. OptiMEM was used to dilute compounds to 6 µM concentration. Cells were treated by adding 50 µL of diluted hsiRNA to 50 µL of cell solution, resulting in a final FBS concentration of 3% and final compound concentration of 3 µM. Compounds were serially diluted in Opti-MEM two-fold within a range of 3

μM to 0 nM, with cells incubated for 1 week. Cells were fed with fresh media without compounds on day 4-5 after treatment.

Treatment of primary neurons with oligonucleotides

mRNA knockdown dose response experiments in mouse primary cortical neurons were carried out as described above with all concentrations as two-fold serial dilutions from 1.5 μM except the 1 μM concentration. Protein knockdown experiments in primary cortical neurons were carried out using the same protocol, but cells were treated with only 1.5 μM compounds. For dSL knockdown experiments in primary cortical neurons, neurons were plated at 1.5E6 per well in 1.5 mL, in 6-well plates pre-coated in poly-L-lysine. In a similar protocol to the above experiments, cells were fed with 1.5 mL media containing antimitotics one day after preparation of cortical cultures, then treated with compounds at a concentration of 1.5 μM for 1 week. Cells were disrupted by pipeting with cold PBS and then pelleted. Cell pellets were processed for dSL quantitation.

mRNA quantification

mRNA was quantified using the QuantiGene 2.0 Assay (Affymetrix; #QS0011) as previously described (Alterman, Coles et al. 2017). Briefly, cells from triplicate wells were lysed in lysis buffer and proteinase K at 55 ^{o}C for thirty minutes and each was mixed thoroughly. Capture plates were prepared by plating 20 μL probe set per well, the appropriate amount of cell lysate as described below, and a volume of diluted lysis mixture such that the total volume of the sample was 100 μL.

For experiments using transgenic neurons, 20 μL of lysate were used to quantitate *hamster* SPTLC1, 40 μL for *mouse* SPTLC1, 20 μL for *mouse* HPRT, 10 μL for *mouse* PPIB. The amounts of lysate used for quantitation were determined by investigating assay linearity (see Supplemental figure S1). Probe sets used for assays in transgenic neurons were species-specific.

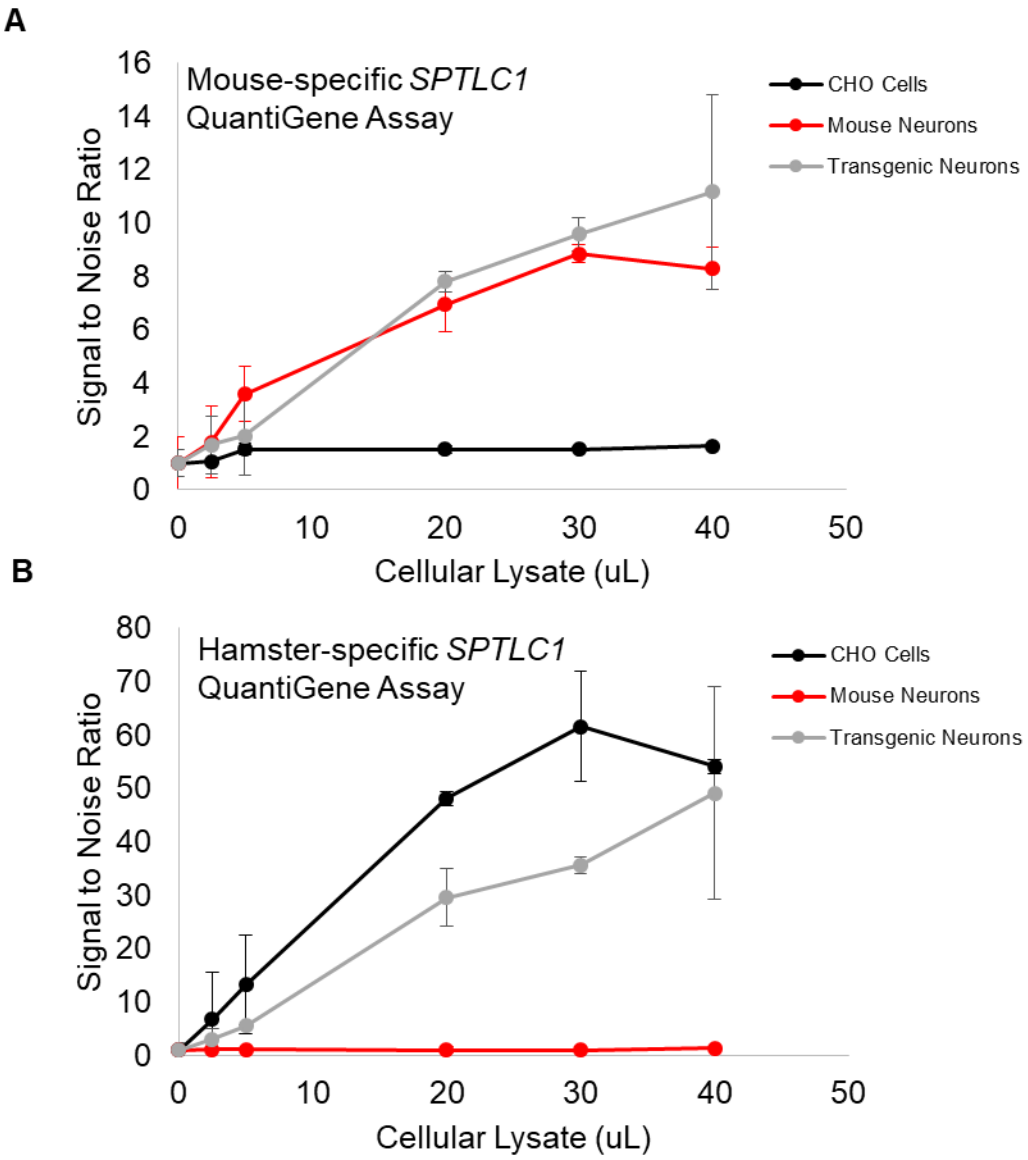

Figure S1. Development and Validation of Assay for Selective Detection of Hamster and Mouse *SPTLC1* mRNA.
CHO cells, wt mouse primary neuron and transgenic mouse primary neuron (expressing hamster C133W *SPTLC1*) lysates were evaluated for SPTLC1 mRNA expression using species-selective QuantiGene Assays, **(A)** mouse specific probe set **(B)** hamster specific probe set. N=2, SD. Signal to Noise was calculated by dividing luminescence of indicated mRNA to background luminescence using either mouse or hamster SPTLC1 probe set.

Dual-Glo Assay for hsiRNA compound screen

Hamster SPTLC1 hsiRNA target sequences were concatenated and a donor oligo was synthesized (IDT Technologies, USA) (Fig. S2). Donor DNA was cloned into psiCHECK2 vector in the 3'UTR of the *Renilla* luciferase gene using restriction sites for AsiS-I and Not-I. HeLa cells plated at 80% confluency were transfected for 6 hours with 24 μg DNA using lipofectamine 2000 transfection reagent diluted in serum-free OptiMEM media, then media was changed to DMEM media supplemented with 10% FBS and 1% penicillin-streptomycin. Cells were trypsinized the following day and plated in a 96-well plate at a density of 10,000 cells/50 μL. Cells were treated with 50 μL of compounds diluted to 1.5 μM for 72 hours. Dual Glo reagents were added as described in the Dual Glo Assay protocol (Promega, USA) and *Renilla* and Firefly luminescence were read (Veritas, Promega, USA). Data were processed by combining the results of two identical experiments of cells treated with each compound in triplicate. For each compound, each of six values of *Renilla* luciferase was divided by its corresponding Firefly luciferase value.

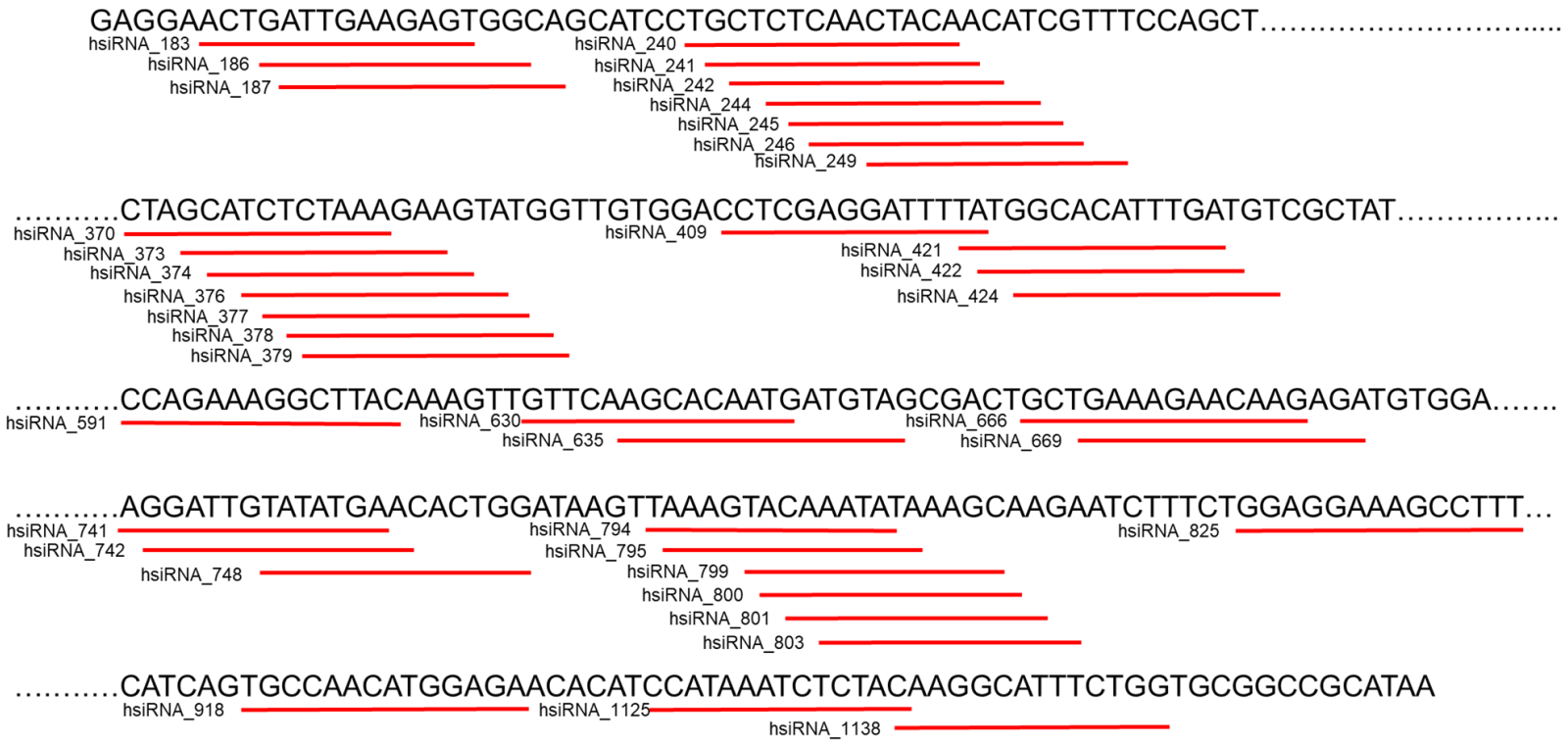

Figure S2. psiCHECK2 donor oligonucleotide contains hsiRNA target sequences
An oligonucleotide containing hsiRNA target sequences was cloned into the psiCHECK2 plasmid in the 3'UTR of the *Renilla* luciferase gene. Target locations of oligonucleotides are shown. This plasmid was used in screening experiments to determine functional hsiRNAs.

Western blot

Westerns were performed using a previously described method (Wright, Huang et al. 2010). Briefly, cell lysates were prepared by lysing cell cultures from a 96 well plate in RIPA buffer and combining material from 6 wells (~600,000 cells per sample). Fifteen μg of total protein from lysates was loaded onto 12% Tris-Glycine gels (Novex, USA) and separated by gel electrophoresis at 120V for 1.5 hours. Proteins were transferred to nitrocellulose membranes and blots were blocked at room temperature for 1-2 hours. Membranes were incubated overnight at 4 ºC with mouse anti-LCB1 (BD Pharmingen, USA), diluted 1:500 and the loading control goat anti-beta actin (Abcam, USA) diluted 1:3000. Mouse and hamster LCB1 protein was normalized to beta actin protein and each sample was compared to untreated within each experiment.

Quantitation of sphingolipids

Sphingolipid content of transgenic embryonic primary cortical neurons was quantitated by LCMS using previously described techniques (Penno, Reilly et al. 2010).

Statistical Analysis

Data were analyzed using GraphPad Prism version 7.04. The log(inhibitor) versus response-variable slope (four parameters) method was used to fit concentration-dependent IC50 curves and calculate IC50 values. For analysis of screening data and protein knockdown data, normality of data was assessed with the D'Agostino-Pearson test. Based on the results (indicating lack of normality and thus the need for non-

parametric statistics), the results of the hsiRNA and ASO screens was evaluated by the Kruskal-Wallis test with Dunn's multiple comparisons test for post-hoc analysis. Other analyses indicated normally distributed data and parametric tests were conducted. Protein knockdown for both mouse and hamster knockdown was assessed separately using a One-Way ANOVA, followed by Dunnett's Multiple Comparisons test to assess group differences from UNT values. Branched DNA assays for mRNA knockdown of hamster and/or mouse SPTLC1 mRNA were evaluated using Two-Way ANOVA.

Results

Design of siRNAs and ASOs for downregulation of hamster and/or mouse SPTLC1. HSAN1 is a monogenic disorder with a toxic gain-of-function mechanism (Penno, Reilly et al. 2010) and thus an ideal candidate for gene silencing strategies including RNAi-based approaches to gene knockdown. McCampbell et al. previously developed and characterized a mouse model of HSAN1 overexpressing the C133W mutant hamster (*hamster*) SPTLC1 transgene in 2005. In this study, we sought to identify siRNAs and ASOs targeting hamster and mouse SPTLC1 to evaluate efficacy and toxicity of these compounds in the context of this model. To this end, we designed a panel of 39 hsiRNAs and 16 LNA Gapmers targeting *hamster* SPTLC1. As the mutant transgene does not contain the 3'UTR, we limited the sequence space to the ORF only. We identified sequences able to target both mouse SPTLC1 and hamster SPTLC1 through analysis of regions with shared mouse/hamster homology, as well as sequences that predicted to target hamster SPTLC1 or mouse SPTLC1 only (Fig. 1). hsiRNA sequences were

developed based on standard siRNA design criteria such as preferring oligonucleotides that have mid-range GC content, absence of miRNA seed sequences, absence of G stretches, and absence of toxic motifs, among other criteria (Birmingham, Anderson et al. 2007).

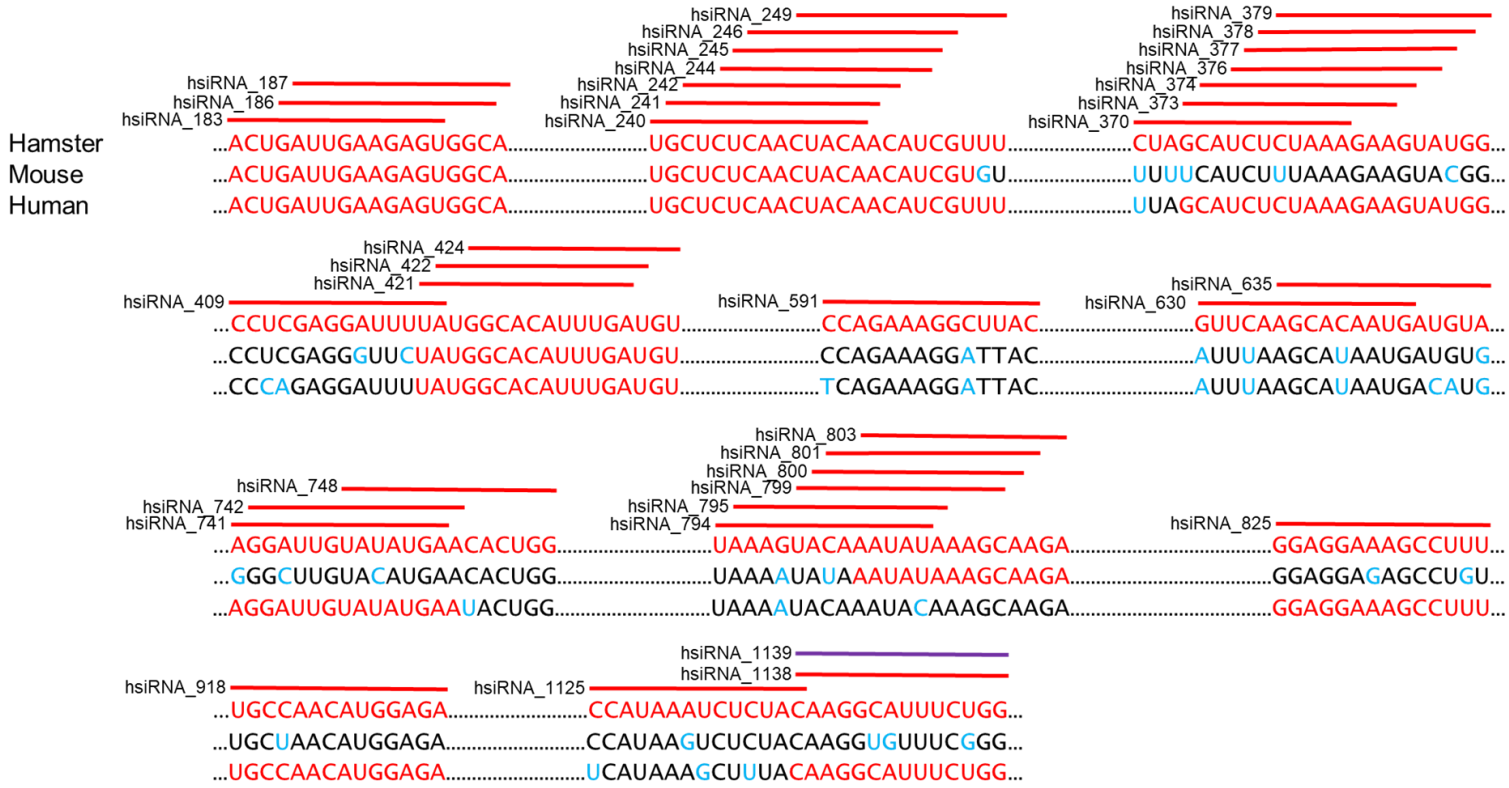

Figure 1. Sequence alignment of hamster, mouse, and human SPTLC1 indicates hsiRNA reagents' target sequences and ability to target different species.

Sequences of hamster, mouse, and human SPTLC1 in relevant regions are shown. All reagents were designed to target hamster SPTLC1 except hsiRNA_1139 (shown in purple), which is designed to target mouse SPTLC1 but does not target hamster or human SPTLC1. Red = targeted, Black = non-targeted, Blue = mismatch.

The asymmetric siRNA scaffold extensively characterized in Dr. Khvorova's lab was used for the screening. The siRNAs have an antisense strand of 20 bases and a sense strand of 15 bases, resulting in the formation of the short duplex region in addition to the fully phosphorothioated tail. An alternating 2′–O–methyl, 2′–fluoro pattern, with a chemically monophosphorylated, 2′–O–methyl–modified uridine (U) at position 1, in combination with terminal phosphorothioated backbone modifications was used to protect from nuclease degradation (Fig. 2a). When conjugated to cholesterol, these compounds efficiently internalize in vitro in all cell types tested without formulation (data not shown) and can silence genes in mice (Alterman, Hall et al. 2015). The exact sequences, chemical configurations, and efficacy of compounds used for screening and initial characterization are shown in Table 1.

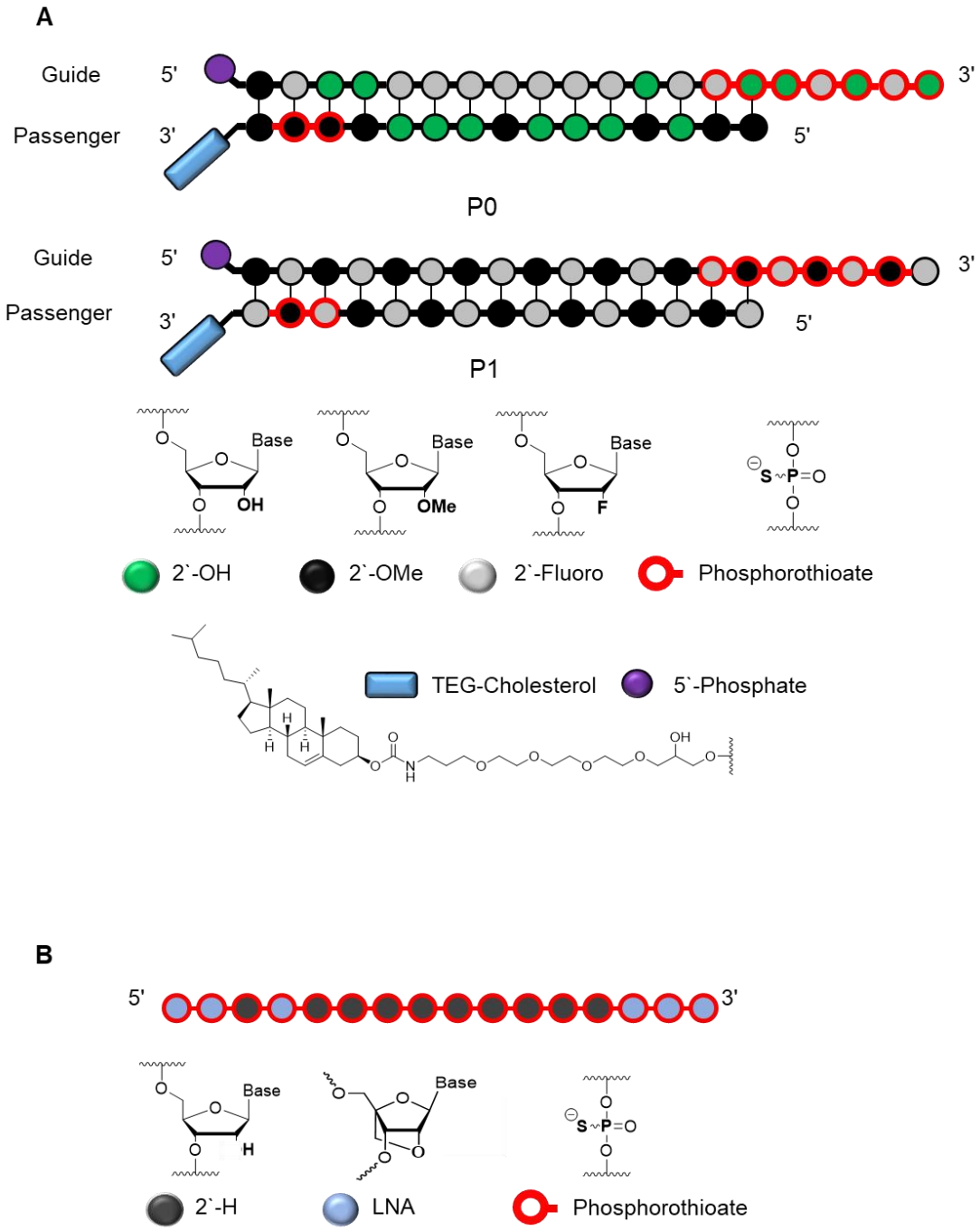

Figure 2. Structure and chemical composition of hsiRNAs and ASOs
(A) hsiRNAs are hydrophobically modified through conjugation of cholesterol and addition of phosphorothioate linkages. 2`-F and 2`-OMe modifications confer nuclease resistance. Two generations of chemical modification patterns were used. **(B)** LNA Gapmers (ASOs) are fully phosphorothioated and contain LNA modifications in regions flanking a central DNA gap

Table 1 Detailed sequence, chemical modification patterns, and efficacy of hsiRNAs targeting hamster SPTLC1

		Strand Modifications					
Gene	**Position**	**Sense Strand**	**Antisense Strand**	**C. griseus**	**M. musculus**	**H. sapiens**	**IC50 Passive Uptake (nM), CHO cells**
hsiRNA_183_P0	183	mA.mC.mU.G.A.mU.mU.G.A.mA.G.A.mG#mU#mA.tegChol	PmU.A.fC.U.fC.U.fU.fC.A.A.fU.fC.A.G#fU#fU#C#fC#fU#C	yes	yes	yes	N/A
hsiRNA_186_P0	186	mG.mA.mU.mU.G.A.mA.G.A.mG.mU.G.G#mC#mA.tegChol	PmU.G.fC.fC.A.fC.U.fC.U.fU.fC.A.A.fU#fC#A#G#fU#fU#C	yes	yes	yes	N/A
hsiRNA_187_P0	187	mA.mU.mU.G.A.mA.G.A.mG.mU.G.G.mC#mA#mA.tegChol	PmU.fU.G.fC.fC.A.fC.U.fC.U.fU.fC.A.A#fU#fC#A#G#fU#U	yes	yes	yes	N/A
hsiRNA_240_P0	240	mU.mG.mC.mU.mC.mU.mC.A.A.mC.mU.A.mC#mA#mA.tegChol	PmU.fU.G.fU.A.G.fU.fU.G.A.mG.A.G.fC#A#G#mG#A#fU#G	yes	yes	yes	N/A
hsiRNA_241_P0	241	mG.mC.mU.mC.mU.mC.A.A.mC.mU.A.mC.A#mA#mA.tegChol	PmU.fU.fU.G.fU.A.G.fU.fU.G.A.mG.A.G#fC#A#G#mG#A#U	yes	yes	yes	N/A
hsiRNA_242_P0	242	mC.mU.mC.mU.mC.A.A.mC.mU.A.mC.A.A#mC#mA.tegChol	PmU.G.fU.fU.G.fU.A.G.fU.fU.G.A.mG.A#G#fC#A#G#mG#A	yes	yes	yes	N/A
hsiRNA_244_P0	244	mC.mU.mC.A.A.mC.mU.A.mC.A.A.mC.A#mU#mA.tegChol	PmU.A.fU.G.fU.fU.G.fU.A.G.fU.fU.G.A#mG#A#G#fC#A#G	yes	yes	yes	N/A
hsiRNA_245_P0	245	mU.mC.A.A.mC.mU.A.mC.A.A.mC.A.mU#mC#mA.tegChol	PmU.G.A.fU.G.fU.fU.G.fU.A.G.fU.fU.G#A#mG#A#G#fC#A	yes	yes	yes	N/A
hsiRNA_246_P0	246	mC.mA.A.mC.mU.A.mC.A.A.mC.A.mU.mC#mG#mA.tegChol	PmU.fC.G.A.fU.G.fU.fU.G.fU.A.G.fU.fU#G#A#mG#A#G#C	yes	yes	yes	N/A
hsiRNA_249_P0	249	mC.mU.A.mC.A.A.mC.A.mU.mC.G.mU.mU#mU#mA.tegChol	PmU.A.A.mA.fC.G.A.fU.G.fU.fU.G.fU.A#G#fU#fU#G#A#G	yes		yes	N/A
hsiRNA_370_P0	370	mC.mU.A.G.mC.A.mU.mC.mU.mC.mU.A.A#mA#mA.tegChol	PmU.fU.U.fU.A.G.mA.G.A.fU.G.fC.fU.A#G#mA#G#fC#fU#G	yes			185
hsiRNA_373_P0	373	mG.mC.A.mU.mC.mU.mC.mU.A.A.mA.G.A#mA#mA.tegChol	PmU.fU.U.fC.U.fU.fU.A.G.mA.G.A.fU.G#fC#fU#A#G#mA#G	yes		yes	N/A
hsiRNA_374_P0	374	mC.mA.mU.mC.mU.mC.mU.A.A.mA.G.A.mA#mG#mA.tegChol	PmU.fC.U.fU.C.fU.U.fU.A.G.mA.G.A.fU#G#fC#fU#A#G#A	yes		yes	448
hsiRNA_376_P0	376	mU.mC.mU.mC.mU.A.A.mA.G.A.mA.G.mU#mA#mA.tegChol	PmU.fU.A.fC.U.fU.fC.U.fU.fU.A.G.mA.G#A#fU#G#fC#fU#A	yes		yes	N/A
hsiRNA_377_P0	377	mC.mU.mC.mU.A.A.mA.G.A.mA.G.mU.A#mU#mA.tegChol	PmU.A.fU.A.fC.U.fU.fC.U.fU.fU.A.G.mA#G#A#fU#G#fC#U	yes		yes	N/A
hsiRNA_378_P0	378	mU.mC.mU.A.A.mA.G.A.mA.G.mU.A.mU#mG#mA.tegChol	PmU.fC.A.fU.A.fC.fU.U.fC.fU.U.fU.A.G#mA#G#A#fU#G#C	yes		yes	N/A
hsiRNA_379_P0	379	mC.mU.A.A.mA.G.A.mA.G.mU.A.mU.G#mG#mA.tegChol	PmU.fC.fC.A.fU.A.fC.U.fU.C.fU.U.fU.A#G#mA#G#A#fU#G	yes		yes	N/A
hsiRNA_409_P0	409	mC.mC.mU.mC.G.A.mG.G.A.mU.mU.mU.mU#mA#mA.tegChol	PmU.fU.A.A.mA.A.fU.fC.C.fU.fC.G.A.mG#G#fU#fC#fC#A#C	yes			N/A
hsiRNA_421_P0	421	mU.mA.mU.G.G.mC.A.mC.A.mU.mU.mU.G#mA#mA.tegChol	PmU.fU.fC.A.A.mA.fU.G.fU.G.fC.fC.A.fU#A#A#mA#A#fU#C	yes	yes	yes	N/A
hsiRNA_422_P0	422	mA.mU.G.G.mC.A.mC.A.mU.mU.mU.G.A#mU#mA.tegChol	PmU.A.fU.fC.A.A.mA.fU.G.fU.G.fC.fC.A#fU#A#A#mA#A#U	yes	yes	yes	N/A
hsiRNA_424_P0	424	mG.mG.mC.A.mC.A.mU.mU.mU.G.A.mU.G#mU#mA.tegChol	PmU.A.fC.A.fU.fC.A.A.mA.fU.G.fU.G.fC#fC#A#fU#A#A#A	yes	yes	yes	N/A
hsiRNA_591_P0	591	mC.mC.A.G.mA.A.A.mG.G.mC.mU.mU.A#mC#mA.tegChol	PmU.G.fU.A.A.mG.fC.C.fU.fU.U.fC.fU.G#G#mA#fU#A#G#C	yes			N/A
hsiRNA_630_P0	630	mG.mU.mU.mC.A.A.mG.mC.A.mC.A.A.mU#mG#mA.tegChol	PmU.fC.A.fU.fU.G.fU.G.fC.fU.fU.G.A.mA#fC#A#A#fC#fU#U	yes			N/A
hsiRNA_635_P0	635	mA.mG.mC.A.mC.A.A.mU.G.A.mU.G.mU#mA#mA.tegChol	PmU.fU.A.fC.A.fU.fC.A.fU.fU.G.fU.G.fC#fU#fU#G#A#mA#C	yes			N/A
hsiRNA_666_P0	666	mG.mC.mU.G.A.mA.A.G.mA.A.mC.A.A#mG#mA.tegChol	PmU.fC.U.fU.G.fU.fU.C.fU.fU.U.fC.A.G#fC#A#G#fU#fC#G	yes			N/A
hsiRNA_669_P0	669	mG.mA.mA.A.G.mA.A.mC.A.A.mG.A.G#mA#mA.tegChol	PmU.fU.C.fU.fC.U.fU.G.fU.fU.C.fU.fU.U#fC#A#G#fC#A#G	yes			749
hsiRNA_741_P0	741	mA.mG.mG.A.mU.mU.G.mU.A.mU.A.mU.G#mA#mA.tegChol	PmU.fU.fC.A.fU.A.fU.A.fC.A.A.fU.fC.C#fU#fU#fC#fC#A#C	yes		yes	780
hsiRNA_742_P0	742	mG.mG.mA.mU.mU.G.mU.A.mU.A.mU.G.A#mA#mA.tegChol	PmU.fU.U.fC.A.fU.A.fU.A.fC.A.A.fU.fC#fC#U#fU#fC#fC#A	yes		yes	N/A
hsiRNA_748_P0	748	mU.mA.mU.A.mU.G.A.mA.mC.A.mC.mU.G#mG#mA.tegChol	PmU.fC.fC.A.G.fU.G.fU.fU.fC.A.fU.A.fU#A#fC#A#A#fU#C	yes			N/A
hsiRNA_794_P0	794	mU.mA.A.mA.G.mU.A.mC.A.A.mA.mU.A#mU#mA.tegChol	PmU.A.fU.A.fU.U.fU.G.fU.A.fC.U.fU.fU#A#A#fC#fU#fU#A	yes			N/A
hsiRNA_795_P0	795	mA.mA.mA.G.mU.A.mC.A.A.mA.mU.A.mU#mA#mA.tegChol	PmU.fU.A.fU.A.fU.U.fU.G.fU.A.fC.U.fU#fU#A#A#fC#fU#U	yes			N/A
hsiRNA_799_P0	799	mU.mA.mC.A.A.mA.mU.A.mU.A.A.mA.G#mC#mA.tegChol	PmU.G.fC.U.fU.fU.A.fU.A.fU.U.fU.G.fU#A#fC#fU#fU#fU#A	yes			N/A
hsiRNA_800_P0	800	mA.mC.A.A.mA.mU.A.mU.A.A.mA.G.mC#mA#mA.tegChol	PmU.fU.G.fC.fU.U.fU.A.fU.A.fU.fU.fU.G#fU#A#fC#fU#fU#U	yes			N/A
hsiRNA_801_P0	801	mC.mA.A.mA.mU.A.mU.A.A.mA.G.mC.A#mA#mA.tegChol	PmU.fU.fU.G.fC.U.fU.fU.A.fU.A.fU.U.fU#G#fU#A#fC#fU#U	yes			N/A
hsiRNA_803_P0	803	mA.mA.mU.A.mU.A.A.mA.G.mC.A.A.mG#mA#mA.tegChol	PmU.fU.fC.U.fU.G.fC.U.fU.fU.A.fU.A.fU#fU#fU#G#fU#A#C	yes	yes		N/A
hsiRNA_825_P0	825	mG.mG.mA.G.G.mA.A.A.mG.mC.mC.mU.mU#mU#mA.tegChol	PmU.A.A.mA.G.G.fC.fU.U.fU.fC.fC.U.fC#fC#A#G#mA#A#A	yes		yes	N/A
hsiRNA_918_P0	918	mU.mG.mC.mC.A.A.mC.A.mU.G.G.mA.G#mA#mA.tegChol	PmU.fU.fC.U.fC.fC.A.fU.G.fU.fU.G.G.fC#A#fC#fU#G#A#U	yes		yes	N/A
hsiRNA_1125_P0	1125	mC.mC.A.mU.A.A.mA.mU.mC.mU.mC.mU.A#mC#mA.tegChol	PmU.G.fU.A.G.mA.G.A.fU.fU.fU.A.fU.G#G#mA#fU#G#fU#G	yes			1074
hsiRNA_1138_P0	1138	mC.mA.A.mG.G.mC.A.mU.mU.mU.mC.mU.G#mG#mA.tegChol	PmU.fC.fC.A.G.mA.A.A.fU.G.fC.fC.fU.fU#G#fU#A#G#mA#G	yes		yes	177

Detailed sequence, chemical modification patterns, and efficacy of hsiRNAs. Chemical modifications are designated as follows. "." – phosphodiester bond, "#" –phosphorothioate bond, "m" – 2'-O-Methyl, "f" – 2'-Fluoro, no prefix – ribonucleotide, "P" – 5' Phosphate, "tegChol" – tetraethylene glycol (teg)-cholesterol. IC50 calculated as described in Materials and Methods. N/A, Not Assessed

Additionally, sixteen LNA Gapmer ASO compounds were designed by Exiqon (USA) using a proprietary algorithm. The ASO scaffold contains a fully phosphorothioated backbone, a central gap of DNA nucleotides, typically flanked by 2-4 LNA (Locked Nucleic Acid) modified nucleotides in varied positions (Fig. 2b). The exact sequences and efficacy of compounds used for screening and initial characterization are shown in Table 2.

Table 2 Detailed sequence, chemical modification patterns, and efficacy of ASOs targeting hamster SPTLC1

		Strand Modifications				
Gene	**Position**	**Sense Strand**	**C. griseus**	**M. musculus**	**H. sapiens**	**IC50 Passive Uptake (nM), CHO cells**
ASO_414	414	T*G*T*G*C*C*A*T*A*A*A*A*T*C*C*T	yes		yes	156
ASO_419	419	T*C*A*A*A*T*G*T*G*C*C*A*T*A*A*A	yes		yes	N/A
ASO_1153	1153	C*C*C*A*C*C*A*C*T*T*T*T*A*A	yes	yes	yes	N/A
ASO_1158	1158	G*G*A*C*T*C*C*C*C*C*A*C*C*A*C*T	yes		yes	N/A
ASO_239	239	T*G*T*A*G*T*T*G*A*G*A*G*C*A*G	yes	yes	yes	N/A
ASO_317	317	A*G*A*A*A*A*T*T*A*A*A*G*G*A*G*G	yes			209
ASO_1141	1141	T*T*A*A*A*C*C*A*G*A*A*A*T*G*C*C	yes			N/A
ASO_415	415	T*G*T*G*C*C*A*T*A*A*A*A*T*C*C	yes		yes	N/A
ASO_138	138	A*C*G*C*T*C*T*T*G*C*A*A*T*T*T*G	yes			101
ASO_813	813	T*C*C*A*G*A*A*A*G*A*T*T*C*T*T	yes			N/A
ASO_258	258	T*G*G*A*G*G*C*C*C*G*G*A*A*A*C*G	yes			N/A
ASO_489	489	A*C*G*A*G*T*A*A*A*T*G*A*T*G	yes	yes		161
ASO_689	689	C*T*C*G*G*A*T*T*C*T*T*T*T*G*A*T	yes			155
ASO_214	214	T*C*G*A*G*A*C*A*G*G*A*G*G*G*A*C	yes			449
ASO_1286	1286	A*A*G*T*A*G*C*G*C*G*C*C*T*G*A*G	yes		yes	3166
ASO_1289	1289	T*C*C*A*A*G*T*A*G*C*G*C*G*C*C*T	yes		yes	146

Detailed sequence, chemical modification patterns, and efficacy of ASOs. Sequences fully phosphorothioated, Exact locations of LNA modifications unknown, proprietary to Exiqon. IC50 calculated as described in Materials and Methods. N/A, Not Assessed

Screen to identify potent siRNAs and ASOs for silencing SPTCL1

An initial screen of 39 hsiRNAs was conducted by dual luciferase assay (Promega, USA). A psiCHECK2 plasmid expressing Firefly luciferase and containing all hsiRNA target sequences cloned into the 3'UTR of the *Renilla* luciferase was pretransfected into HeLa cells. hsiRNAs targeting *hamster* SPTLC1 were then passively transfected into HeLa cells at a concentration of 1.5 μM. Using this experimental design, efficacy of hsiRNAs can be quantified by comparing the ratios of *Renilla*/Firefly luciferase of each hsiRNA to the ratio of *Renilla*/Firefly luciferase of untreated cells. Two identical screening experiments were performed, each with triplicate wells. One screen exhibited a hit rate of 25.6% while the other had a hit rate of 15.4%, for compounds silencing the gene to less than 50% of untreated controls. Of these lead compounds, four were common among the two screens. Additionally, three compounds in the first screen and two compounds in the second screen silenced their SPTLC1 targets by ~70% or more (Fig. S3). Statistical analysis of data from both screens together indicated that seven compounds were able to significantly downregulate their targets as determined by reduction in relative bioluminescence (*Renilla*/Firefly luminescence) (Fig. 3a). Additionally, several compounds exhibited toxicity as indicated by low firefly luciferase expression (data not shown). The two lead compounds chosen were hsiRNA_374 and hsiRNA_1138, which averaged 77.9% and 76.8% knockdown, respectively.

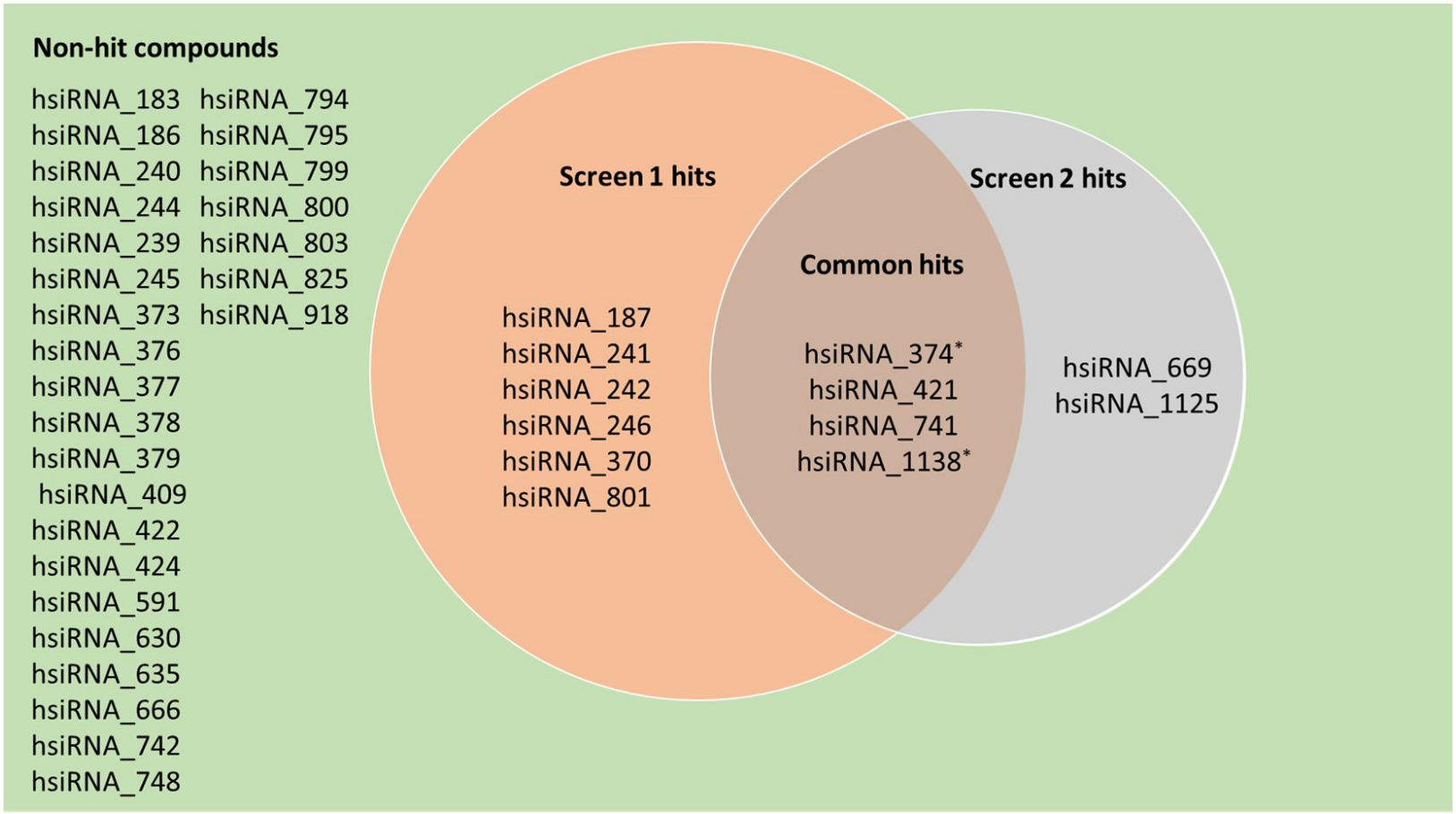

Figure S3. hsiRNA screen results reveal four common lead compounds
Two identical hsiRNA screens were conducted by transfection of HeLa cells with psiCHECK2 plasmid containing hsiRNA target sequences cloned into 3'UTR of *Renilla* luciferase gene. Cells were then treated with compounds at 1.5 μM concentration for 72 hours, then *Renilla* and firefly luciferase luminescence were detected. *Renilla*/firefly luciferase expression was expressed as a percent of untreated cells and lead compounds were identified as compounds a reduction in *Renilla*/firefly luminescence as compared to untreated of more than 50% (n=3 per experiment). Four common lead compounds were identified. *, compounds reduced *Renilla*/firefly luminescence to less than 30% in both screens.

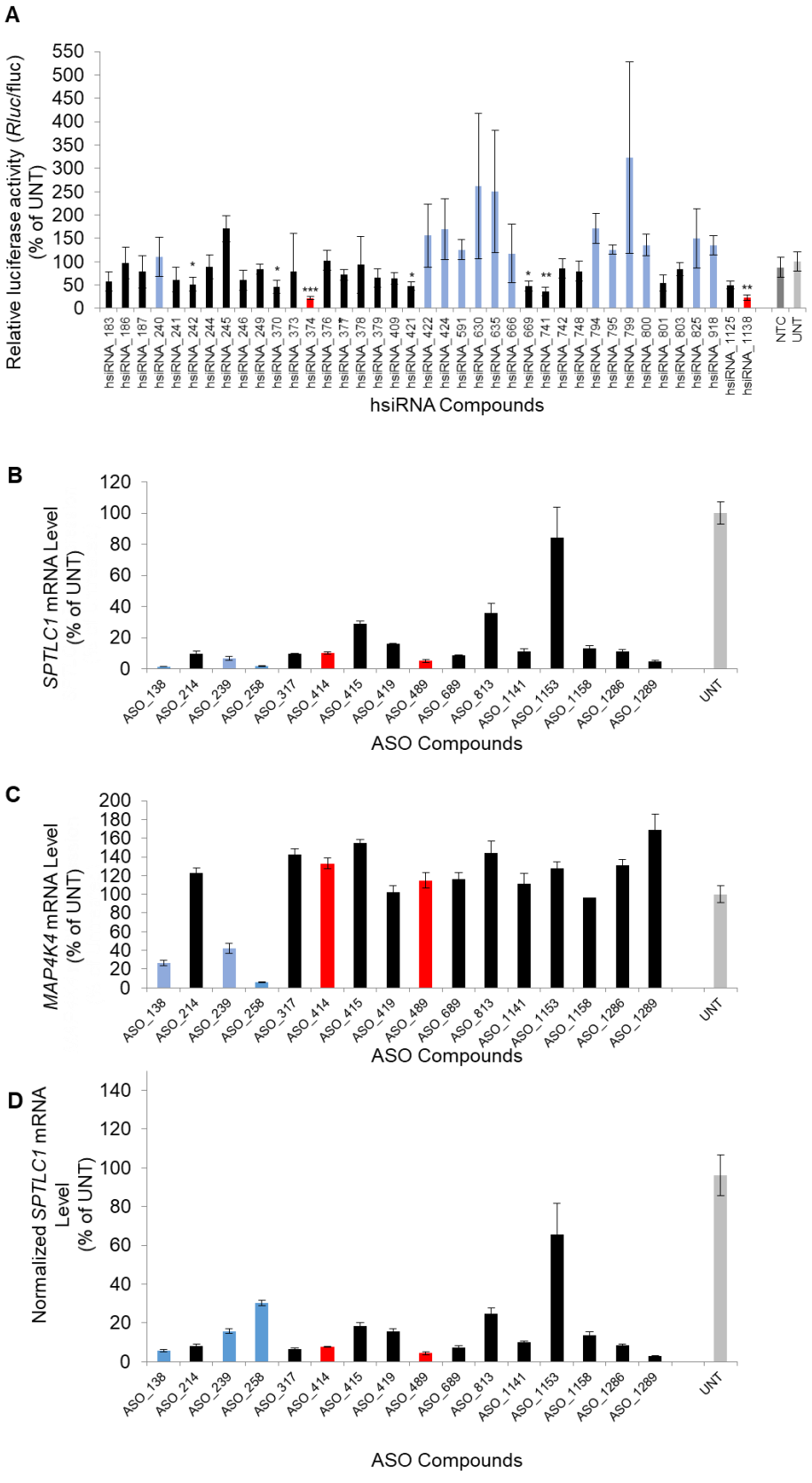
A
Relative luciferase activity (*Rluc*/fluc) (% of UNT)
550
500
450
400
350
300
250
200
150
100
50
0
hsiRNA_183
hsiRNA_186
hsiRNA_187
hsiRNA_240
hsiRNA_241
hsiRNA_242
hsiRNA_244
hsiRNA_245
hsiRNA_246
hsiRNA_249
hsiRNA_370
hsiRNA_373
hsiRNA_374
hsiRNA_376
hsiRNA_377
hsiRNA_378
hsiRNA_379
hsiRNA_409
hsiRNA_421
hsiRNA_422
hsiRNA_424
hsiRNA_591
hsiRNA_630
hsiRNA_635
hsiRNA_666
hsiRNA_669
hsiRNA_741
hsiRNA_742
hsiRNA_748
hsiRNA_794
hsiRNA_795
hsiRNA_799
hsiRNA_800
hsiRNA_801
hsiRNA_803
hsiRNA_825
hsiRNA_918
hsiRNA_1125
hsiRNA_1138
NTC
UNT
hsiRNA Compounds
B
SPTLC1 mRNA Level (% of UNT)
120
100
80
60
40
20
0
ASO_138
ASO_214
ASO_239
ASO_258
ASO_317
ASO_414
ASO_415
ASO_419
ASO_489
ASO_689
ASO_813
ASO_1141
ASO_1153
ASO_1158
ASO_1286
ASO_1289
UNT
ASO Compounds
C
MAP4K4 mRNA Level (% of UNT)
200
180
160
140
120
100
80
60
40
20
0
ASO_138
ASO_214
ASO_239
ASO_258
ASO_317
ASO_414
ASO_415
ASO_419
ASO_489
ASO_689
ASO_813
ASO_1141
ASO_1153
ASO_1158
ASO_1286
ASO_1289
UNT
ASO Compounds
D
Normalized *SPTLC1* mRNA Level (% of UNT)
140
120
100
80
60
40
20
0
ASO_138
ASO_214
ASO_239
ASO_258
ASO_317
ASO_414
ASO_415
ASO_419
ASO_489
ASO_689
ASO_813
ASO_1141
ASO_1153
ASO_1158
ASO_1286
ASO_1289
UNT
ASO Compounds

Figure 3. Identification of hsiRNA and ASO Compounds for Silencing of Hamster *SPTLC1* mRNA.

(A) HeLa cells were pre-transfected with psiCHECK2 plasmid containing targeted regions of SPTLC1 mRNA cloned in the 3'UTR. A panel of hsiRNAs was added to cells (no transfection reagent) at 1.5 uM concentration 24 hours post plasmid transfection. hsiRNA efficacy is evaluated at 72 hours post treatment using DualGlo Assay (Promega). N=6, SD, NTC- Non Targeting Control, UNT- Untreated Cells. Toxic compounds, shown in blue, exhibited low firefly luciferase expression.

(B), (C) CHO cells were treated with 100 nM ASOs complexed with RNAiMax transfection reagent. ASO efficacy was evaluated at 72 hours post treatment using QuantiGene Assay. Panel (**B**) shows SPTLC1 mRNA expression, panel (**C**) shows housekeeping gene expression (MAP4K4), and (**D**) shows SPTLC1 normalized to MAP4K4 expression. N=3, SD, UNT- Untreated Cells. Toxic compounds exhibited low MAP4K4 expression.

Legend: Blue = Toxic Compound, Black = Inactive Compound, Red = Lead Compound. *, $P \leq 0.05$; **, $P \leq 0.01$; ***, $P \leq 0.001$

Similarly, 16 LNAs were screened by treating CHO cells with compounds at a concentration of 100 nM for 72 hours. Compounds were delivered by lipid transfection and their efficacy assessed by branched DNA Assay (Quantigene, Affymetrix) 15 out of 16 of the compounds silenced hamster by more than ~70%, with nine compounds silencing by more than 90%. However, three of these compounds exhibited toxicity as indicated by reduced expression of MAP4K4, the housekeeping gene, relative to untreated controls (Fig. 3b,c). Compounds ASO_414, ASO_489, and ASO_1289 were the top hits, with efficacies of 92.3, 95.6, and 97.3%, respectively (Fig. 3d). In subsequent experiments (data not shown), ASO_1289 was shown to be ineffective at silencing SPTLC1, and ASO_414 and ASO_489 were identified as the top leads.

Lead ASOs and hsiRNAs efficiently and potently knock down *hamster* SPTLC1 and vary in ability to knock down *mouse* SPTLC1

The two lead hsiRNA compounds, hsiRNA_1138 and hsiRNA_374, as well as the lead two LNA Gapmer compounds were further characterized by conducting dose response assays in CHO-K1 cells to evaluate the compounds' ability to target endogenous *hamster* SPTLC1. Compounds were passively transfected into cells at concentrations varying from 50 nM to 3 μM (Fig. 4a,b). The two hsiRNA lead compounds appeared to have similar efficacies, with hsiRNA_1138 having an IC50 of 359 nM, compared to hsiRNA_374, which had an IC50 of 448 nM. The two lead ASO compounds, ASO_414 and ASO_489, were equally potent with an IC50 of 155 nM, while ASO_414 appeared slightly more efficacious than ASO_489 (Fig. 4a, b).

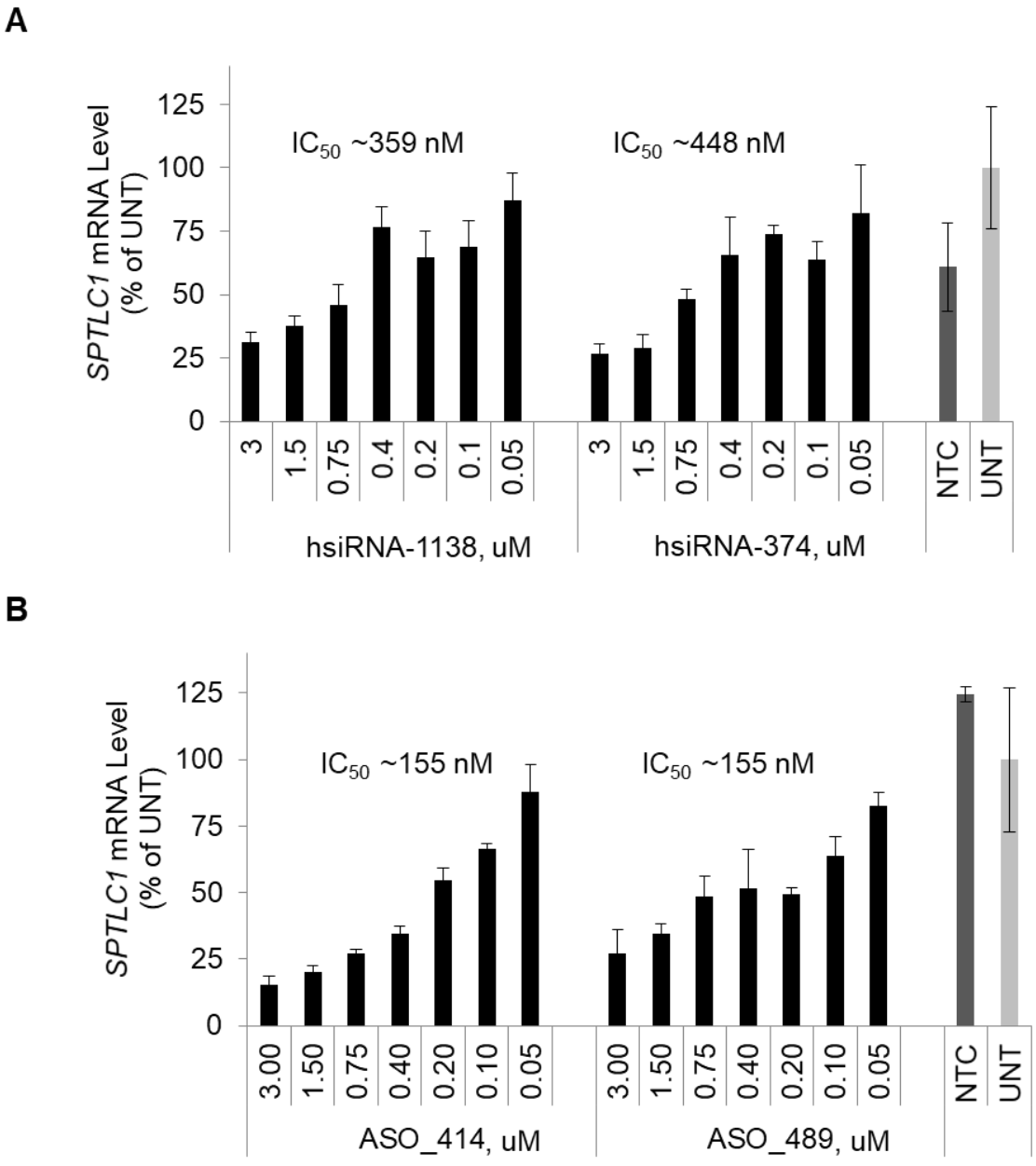

Figure 4. Validation of hsiRNA and ASO Lead Compounds for Silencing of Hamster *SPTLC1* mRNA in CHO cells.
CHO cells were treated with different concentrations (passive transfection) of hsiRNAs **(A)** or ASOs **(B)** Compound potency was evaluated at 72 hours post treatment using QuantiGene Assay. N=3, SD, NTC- Non Targeting Control, UNT- Untreated Cells.

We also evaluated these compounds' ability to target *mouse* SPTLC1, again by passive transfection at concentrations varying from 50 nM to 3 μM, but this time in mouse primary cortical neurons. Both hsiRNA_1138 (Fig. 5a) and hsiRNA_374 (data not shown) did not have the ability to target *mouse* SPTLC1. In order to complete our catalogue of compounds, we developed and synthesized a panel of hsiRNA compounds targeting *mouse* SPTLC1 only, by using the *mouse* –targeting sequences corresponding to the position of the top *hamster*-targeting sequences. We evaluated these compounds by branched DNA assay and identified hsiRNA-1143 as a hit compound with the ability to robustly target *mouse* SPTLC1. ASO_489 was able to robustly target *mouse* SPTLC1 while ASO_414 silenced mouse SPTLC1 but displayed low potency and appeared to have lower efficacy (Fig. 5b). A summary of sequences, chemical modifications, and homology for each lead compound is shown in Table 3.

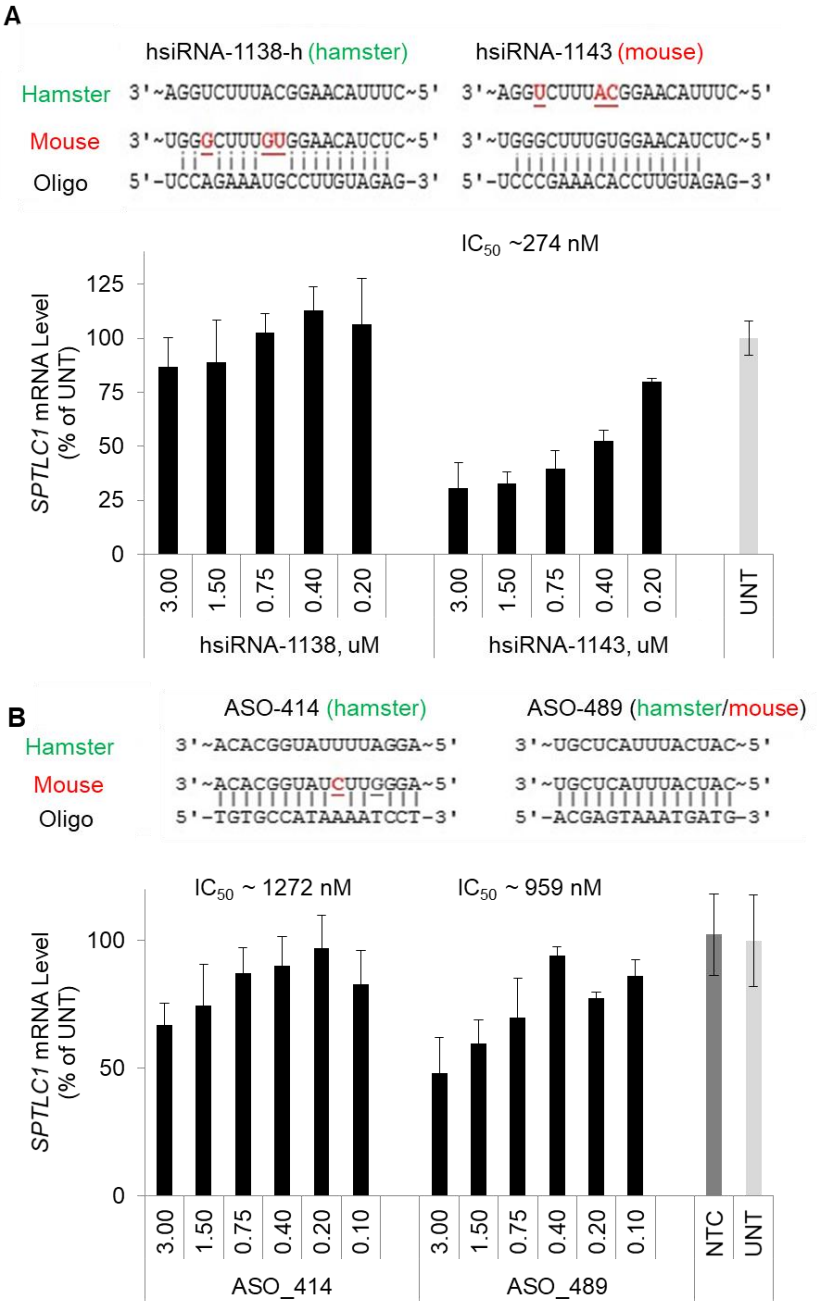

Figure 5. Validation of hsiRNA and ASO Lead Compounds for Silencing of Mouse *SPTLC1* mRNA in Mouse Primary Cortical Neurons.
Mouse primary neurons were treated with different concentrations (passive transfection) of hsiRNAs **(A)** or ASOs **(B).** Compound potency was evaluated at 72 hours post treatment using QuantiGene Assay. N=3, SD, NTC- Non Targeting Control, UNT- Untreated Cells. Compounds hsiRNA_1138 and ASO_414 have mismatches with mouse *SPTLC1* mRNA and thus are inactive.

Table 3 Detailed sequence, chemical modification patterns of lead hsiRNAs and ASOs targeting SPTLC1

		Strand Modifications				
Gene	**Position**	**Sense Strand**	**Antisense Strand**	**C. griseus**	**M. musculus**	**H. sapiens**
hsiRNA_374_P1	374	fC.mA.fU.mC.fU.mC.fU.mA.fA.mA.fG.mA.fA#mG#fA.tegChol	PmU.fC.mU.fU.mC.fU.mU.fU.mA.fG.mA.fG.mA.fU#mG#fC#mU#fA#mG#fA	yes		yes
hsiRNA_1138_P1	1138	fC.mA.fA.mG.fG.mC.fA.mU.fU.mU.fC.mU.fG#mG#fA.tegChol	PmU.fC.mC.fA.mG.fA.mA.fA.mU.fG.mC.fC.mU.fU#mG#fU#mA#fG#mA#fG	yes		yes
hsiRNA_1143_P1	1143	fC.mA.fA.mG.fG.mU.fG.mU.fU.mU.fC.mG.fG#mG#fA.tegChol	PmU.fC.mC.fC.mG.fA.mA.fA.mC.fA.mC.fC.mU.fU#mG#fU#mA#fG#mA#fG		yes	
ASO_414	414	T*G*T*G*C*C*A*T*A*A*A*A*T*C*C*T		yes		yes
ASO_489	489	A*C*G*A*G*T*A*A*A*T*G*A*T*G	yes	yes		161

Detailed sequence, chemical modification patterns, and efficacy of hsiRNAs. Chemical modifications are designated as follows. "." – phosphodiester bond, "#" –phosphorothioate bond, "m" – 2'-O-Methyl, "f" – 2'-Fluoro, no prefix – ribonucleotide, "P" – 5' Phosphate, "tegChol" – tetraethylene glycol (teg)-cholesterol. Exact locations of LNA modifications unknown, proprietary to Exiqon. IC50 calculated as described in Materials and Methods. N/A, Not Assessed

Lead ASOs and hsiRNAs potently and differentially knock down *hamster* SPTLC1 and *mouse* SPTLC1 mRNA in an in vitro model of HSAN1

After we established the lead compounds' differential ability to silence mutant hamster vs wild type mouse SPTLC1 when only one species of transcript is present, our next goal was to test this in an in vitro model system of HSAN1, which expresses both hamster and mouse SPTLC1. We did this by culturing primary embryonic cortical neurons from pregnant wild type females that were crossed with transgenic males. These cultures had sufficient expression of both mutant hamster SPTLC1 and wild type mouse SPLTC1 to be able to detect knockdown by the lead compounds (data not shown). We developed a species-specific assay to detect differential expression and knockdown of both transcripts using the branched DNA assay. We then investigated whether the lead compounds induced species selective dose-dependent inhibition of transcript levels in these cultures. Compounds were administered by passive delivery at a range of concentrations, from 50 nM to 3 μM. Among the hsiRNA compounds, hsiRNA_1138 shows selective reduction of hamster SPTLC1 (Fig. 6a), while hsiRNA_1143 (Fig. 6b) shows selective reduction of mouse SPTLC1. These hsiRNAs are potent, with IC50s in the 100-300 nM range. Among the ASOs, both ASO_414 and ASO_489 downregulate both hamster and mouse SPLTC1. ASO_414 , however, shows greater ability to target hamster SPTLC1 than mouse SPTLC1, as evidenced by a lower IC50. The exact IC50 for ASO_414 as determined from best fit nonlinear regression is not reliable as this compound is highly effective throughout the range of concentrations tested, but we can conclude it is less than 50 nM.

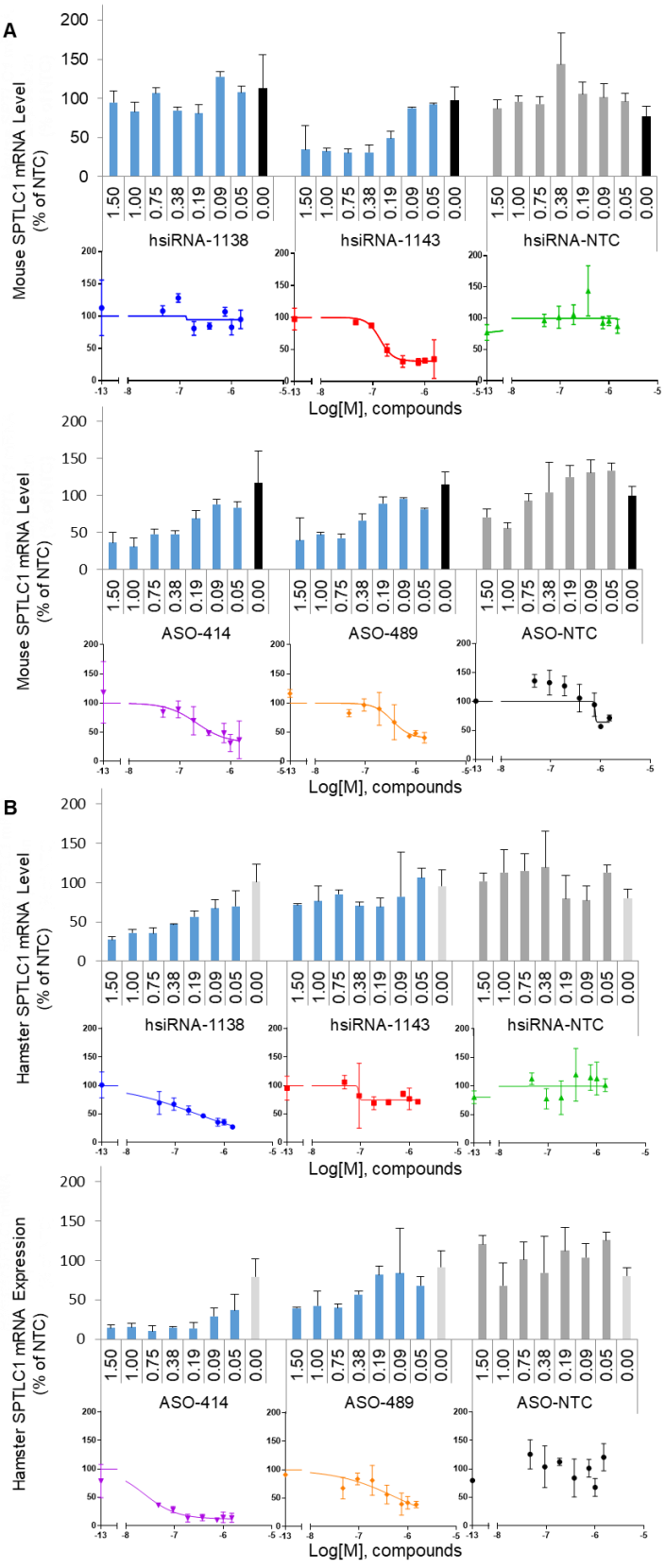

	IC50, uM
Expt ID	hsiRNA-1143
170616	112.5
170619	137.4
170807	300.2
Average	183.4

	IC50, uM	
Expt ID	ASO-414	ASO-489
170616	161.0	363.7
170619	215.8	343.8
170807	89.6	377.9
Average	155.5	361.8

	IC50, uM
Expt ID	hsiRNA-1138
170616	231.2
170619	235.9
170807	127.4
Average	198.2

	IC50, uM
Expt ID	ASO-489
170616	102.2
170619	548.9
170807	56.5
Average	235.9

ASO-414: EC50 < 50nM

Figure 6. Selective Silencing of Hamster and Mouse SPTLC1 mRNA in C133W Transgenic Primary Neurons.
C133W neurons were treated with hsiRNAs and ASOs at a range of concentrations from 1.5 μM to 50 nM. Level of Mouse **(A)** and Hamster **(B)** SPTLC1 mRNA determined at 1 week with Quantigene assay, shown with respect to [μM] in bar graphs and log[M] in linear regression curves. N=3, SD, NTC- Non Targeting Control, UNT- Untreated Cells. IC50 values are shown.

Lead ASOs and hsiRNAs potently and differentially knock down hamster LCB1 and mouse LCB1 protein in an in vitro model of HSAN1

Next, we investigated whether reduction of LCB1 protein mirrored reduction of SPTLC1 mRNA and whether the knockdown remained species-specific based on the compound used. We treated primary cortical neurons from transgenic animals for 1 week with the lead compounds at a concentration of 1.5 μM. We found that hsiRNA_1138, ASO_414, and ASO_489, all showed significant reduction of hamster LCB1 levels, while ASO_414, ASO_489, and the mouse-selective hsiRNA_1143 all showed a trend towards reduction in mouse LCB1 protein levels that was not significant (Fig. 7a, b). ASO_414 showed the most potent silencing of hamster protein, knocking it down by 85%, while hsiRNA_1143 was the most potent reagent reducing mouse LCB1 protein, silencing it by ~50%.

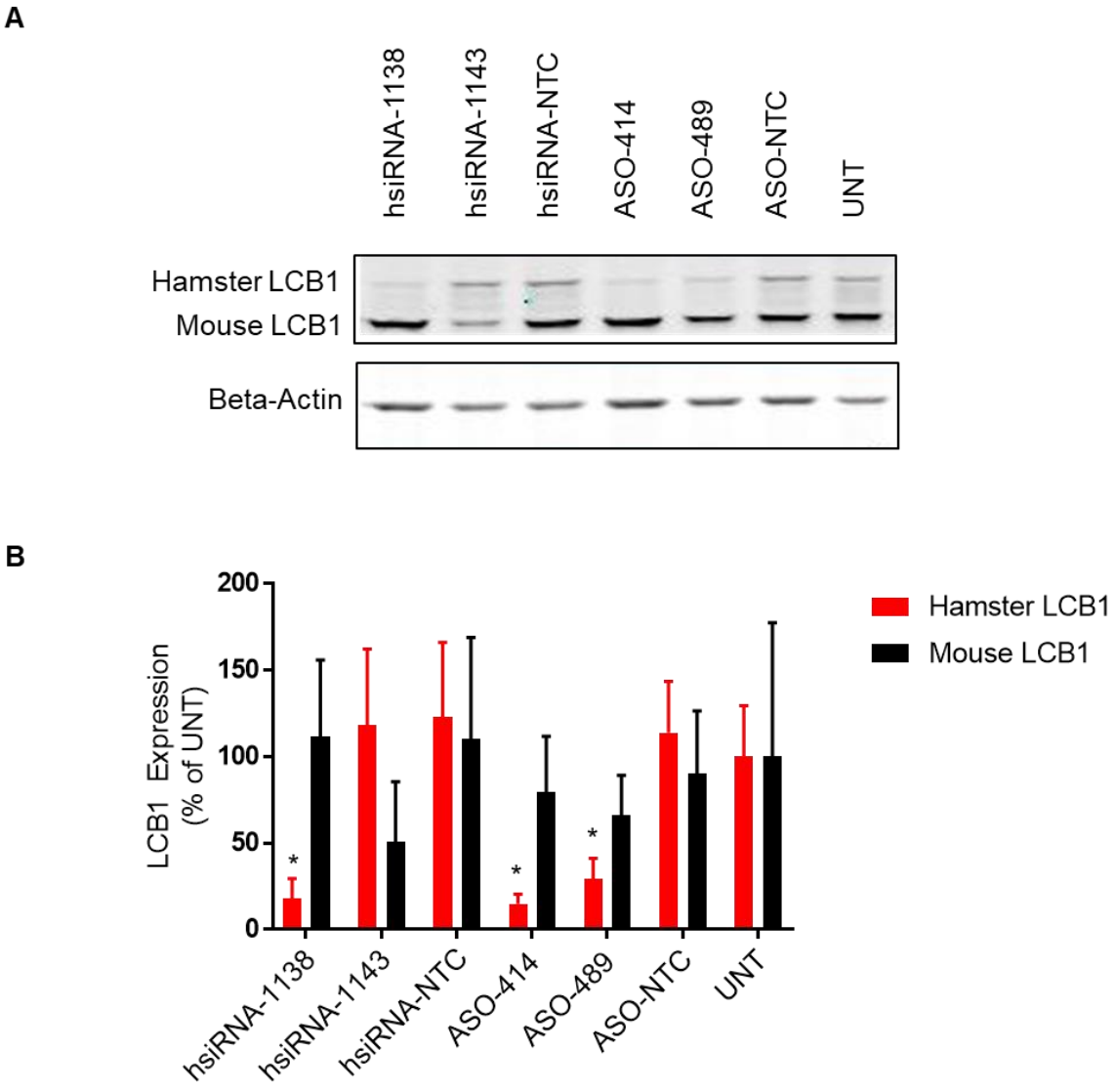

Figure 7. Selective Silencing of Hamster and Mouse LCB1 Protein in C133W Transgenic Primary Neurons.

C133W neurons were treated with hsiRNAs and ASOs at 1.5 μM concentration. **(A)** Level of hamster and mouse LCB1 protein determined at 1 week by western blot and quantified by densitometry **(B)**. N=5, SD, NTC-Non Targeting Control, UNT- Untreated Cells. *, $P \leq 0.05$

Lead ASOs and hsiRNAs do not impact dSL production in an in vitro model of HSAN1

In addition to demonstrating potent silencing of SPTLC1 mRNA and protein, we also tested the ability of the lead compounds to reduce production of dSLs, which are thought to be the causative agent of disease in HSAN1. We cultured transgenic primary neurons and wild type primary neurons and compared their sphingolipid profiles (Fig. 8a). We found that dSLs are indeed expressed in such cultures and they are produced at levels that allow detection of knockdown should it occur. Specifically, doxSO and doxSA are present in transgenic cultures at average levels of 0.046 and 0.026 pmol/ug, respectively, when normalized to the internal standard d7SO. These species were not detectable in wild type cultures.

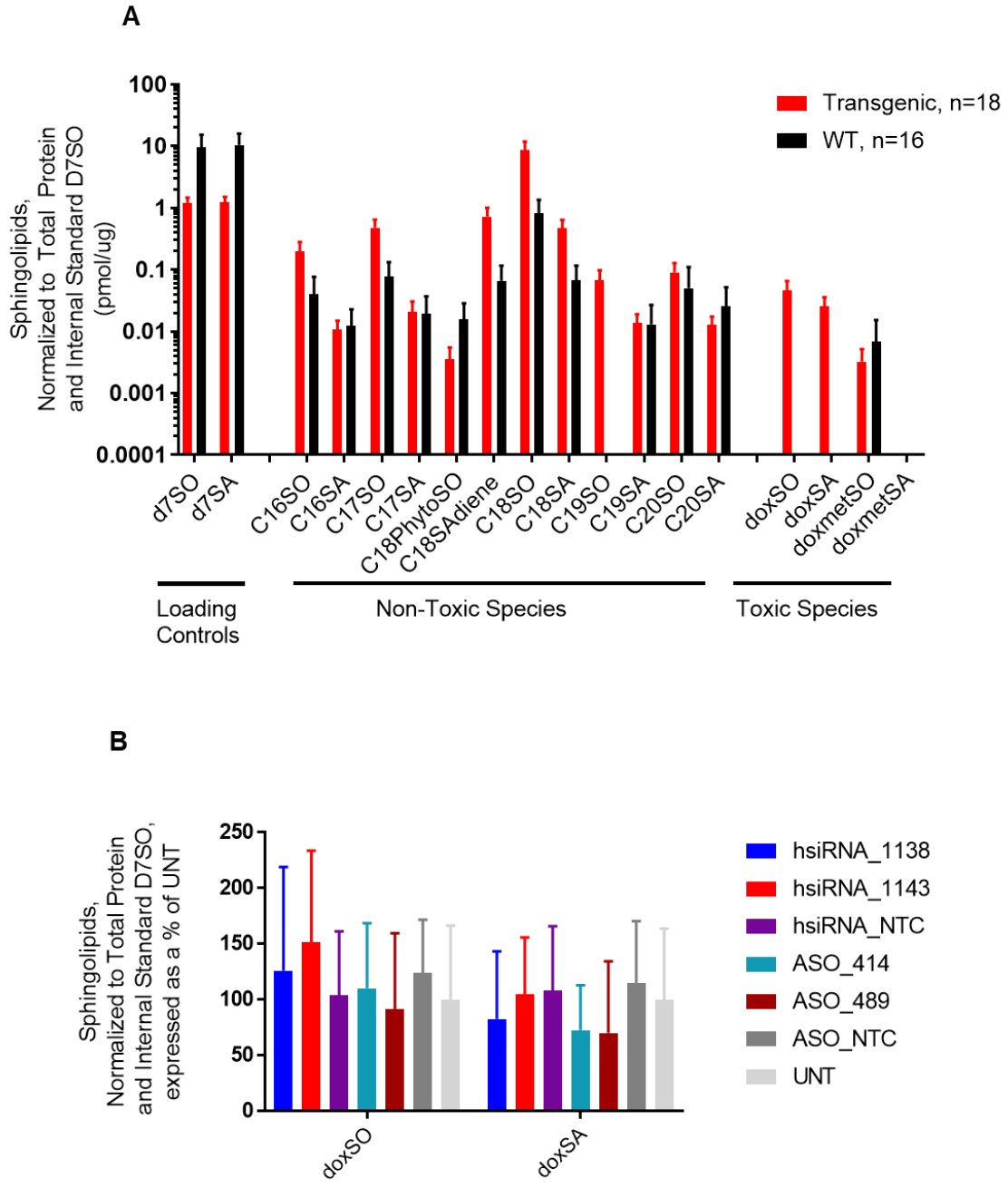

Figure 8. Primary Cortical Neuron Cultures Produce dSLs
(A) Sphingolipid profiles of transgenic and wild type primary cortical neurons cultured for 1 week were assessed and doxSO and doxSA were identified as toxic species that accumulate in transgenic cultures but not in wild type cultures. (B) C133W Neurons were treated with hsiRNAs and ASOs at 1.5 μM concentration. Level of toxic species doxSO and doxSA were quantitated at 1 week by mass spectrometry. A trend towards reduction of doxSA by hamster-targeting compounds can be seen. N=6, SD, NTC- Non Targeting Control, UNT- Untreated Cells.

We then treated primary cortical neurons isolated from transgenic mice for 1 week with our lead compounds at a concentration of 1.5 μM. We found a high degree of variability in dSLs among all samples tested, including untreated. Thus we cannot conclude that there is any difference between treatment with hamster-targeting compounds and untreated or NTC groups (Fig. 8b).

Discussion

HSAN1 is a debilitating, autosomal dominantly inherited, neurological disorder resulting in a progressive polyneuropathy primarily affecting pain and temperature sensation in the distal limbs (Penno, Reilly et al. 2010). Complications such as amputation and skin and bone infections considerably impact patients' quality of life (Auer-Grumbach 2008). Thus far, there are no FDA-approved treatments for this disease (Eichler 2018). A Phase II clinical trial is underway investigating the impact of oral L-serine supplementation on disease progression and reversibility of symptoms (Eichler 2017). As a monogenic disorder in which the mutants have a well-described acquired toxic property (production of dSLs), HSAN1 is a prime candidate for RNAi-based gene silencing strategies. In that vein, we selected two classes of compounds that have enjoyed recent success in clinical development, siRNAs and ASOs, to investigate their ability to downregulate the causative gene in HSAN1, SPTLC1.

Screening and Validation of Lead Compounds

We designed and screened a panel of 39 hsiRNAs and 16 ASOs that target hamster SPTLC1, which is overexpressed in the C133W transgenic mouse model. Our hsiRNA screens exhibited hit rates of 25.6% and 15.4%, and the ASO compounds showed a much higher hit rate than the hsiRNA screens. On further characterization of the compounds, the ASOs tested showed higher potency in CHO cells, with IC50s in the 100 nM range, while the hsiRNAs tested were less potent, with IC50s in the 400 nM range. In mouse primary neurons, however, the hsiRNA chemistry had a higher potency, with hsiRNA_1143 exhibiting a lower IC50 relative to ASO_489 and ASO_414. This discrepancy is a result of the fact that hsiRNA-1143 was designed specifically to target mouse SPTLC1 whereas ASO_489 had a lower efficacy when tested in CHO-K1 cells and ASO_414 was not expected to target mouse SPTLC1 at all since it contains a mismatch. We also established the species-specific nature of the lead compounds, with hsiRNA_1138 being hamster-selective and hsiRNA_1143 being mouse-selective. ASO_489 as anticipated was able to target both hamster and mouse SPTLC1, while ASO_414 was able to target hamster SPTLC1 in CHO cells and unable to potently target mouse SPTLC1 in wt mouse primary cortical neurons.

We then demonstrated species-specificity in an in vitro model of HSAN1, transgenic primary cortical neuron cultures, expressing both hamster and mouse SPTLC1. We assessed the differential capacity of our lead compounds to knockdown mRNA, protein, and toxic dSLs.

mRNA Knockdown Analysis

With regard to mRNA knockdown analysis, two experiments were excluded from the analysis, as they exhibited a marked central plate effect. The plate effect could arise due to loose sealing of branched DNA assay plates, which could result in evaporation from the outside wells. Since these experiments demonstrated a plate effect consisting of a marked variation in luminescence in the outside wells as compared to central wells, they were excluded from analysis, as is the standard practice in the Khvorova lab. The three experiments indicated were used in the analysis.

Our data indicate that the lead compounds retained their species-specificity with respect to mRNA downregulation as compared to their activity in CHO-K1 cells and wild type mouse primary cortical neurons. hsiRNA_1138, ASO_414, and ASO_489 all silence hamster SPTLC1 as expected, while hsiRNA_1143, ASO_414, and ASO_489 all silence mouse SPTLC1. As mentioned, ASO_414 was not designed to target mouse SPTLC1, but appeared efficacious in wild type mouse primary cortical neurons. This effect was amplified in transgenic mouse primary cortical neurons. A possible explanation for this situation is that the ASO_414 compound became contaminated by the ASO_489 compound. Nevertheless, ASO_414 clearly shows higher potency in silencing hamster SPTLC1 as compared to mouse SPTLC1, as the IC50 of ASO_414 for hamster SPTLC1 is less than 50 nM (beyond the limit of detection for the range of concentrations tested).

Notably, there is a high degree of variability in the IC50 values between experiments. This could be due to the fact that each experiment is conducted on a separate batch of

primary neurons, derived from a different pregnant mouse. Since the wild type females are crossed with males that are heterozygous for the transgene, each pregnant mouse will have embryos that are heterozygous transgenic and wild type. Neurons from all embryos are used to prepare cortical neuron cultures, so there is a different ratio of transgenic to wild type neurons in every culture prepared. Thus, even though the transgene is generally highly expressed, the level of expression may vary between cultures. Additionally, the level of wild type mouse SPTLC1 is lower in transgenic neurons than in wild type neurons (data not shown). This may indicate the existence of a negative feedback mechanism which regulates the overall abundance of SPTLC1 mRNA, whether transgenic or wild type, such that it does not become too high. Thus there may be a high degree of variability of both mouse SPTLC1 and hamster SPTLC1 between these transgenic cultures, and this may contribute to the high degree of variability observed in IC50 values. Still, the general observations are well-supported among all experiments that hsiRNA_1138, ASO_414, and ASO_489 silence hamster SPTLC1, while hsiRNA_1143, ASO_414, and ASO_489 silence mouse SPTLC1.

Additionally, there appears to be a high degree of variability in some experiments among the mRNA levels of untreated cells. This could be due to differential ratios of transgenic to wild type neurons within individual wells of the culture plate if cultures were not entirely homogenous when plated. Thus, we chose to normalize data to the more numerous readings from NTC wells instead of normalizing to the few untreated wells. This may also complicate interpretation of the results and IC50s of the lead compounds.

A more optimal experimental design might entail preparing primary cortical neuron cultures from individual embryos and testing compounds in cultures derived from only heterozygous transgenic embryos in order to minimize these key sources of variability. Another option would be to generate a mouse homozygous for the transgene and cross this mouse with a wild type mouse, thus ensuring all resulting embryos are heterozygous.

Protein Knockdown Analysis

The next step was to investigate whether the species selectivity displayed by our reagents with respect to mRNA was preserved with respect to protein. We found that just as in mRNA, hsiRNA_1138, ASO_414, and ASO_489 are able to silence hamster LCB1, while hsiRNA_1143, ASO_414, and ASO_489 reduce mouse LCB1. However, the hamster-targeting reagents produce a greater degree of silencing than do the mouse-targeting reagents. This difference cannot be explained by efficacy. Compound hsiRNA_1139, which had comparable efficacy to ASO_414 in silencing mRNA in both wild type and transgenic primary neuron cultures, is unable to silence wild type mouse LCB1 protein to the same extent that ASO_414 can reduce hamster LCB1 protein. One potential explanation for this difference in protein silencing is that there is instability of the hamster LCB1 protein. Previous work has shown that mutant LCB1 protein levels are reduced compared to wild type protein in other lines of C133W HSAN1 mice developed, such as 8B and 8F, while the mutant mRNA is expressed at a level equal to endogenous SPTLC1 mRNA(McCampbell, Truong et al. 2005). Moreover, our findings

indicate that there is a more consistent downregulation of LCB1 protein than SPTLC1 mRNA. Another factor influencing interpretation of these data is the high degree of variability of mouse LCB1 protein expression in untreated cells. If less variability of mouse LCB1 protein was observed in untreated cells, the silencing capability of hsiRNA_1143 may have reached statistical significance, although it would remain less effective at silencing mouse LCB1 than the hamster-targeting compounds were at targeting hamster LCB1.

dSL Knockdown Analysis

The robust knockdown observed in mRNA and protein after treatment with our lead hamster-targeting compounds did not result in a reduction of dSLs. One issue is that our assay to validate doxSO and doxSA as potential markers to distinguish between transgenic cultures and wild type cultures and to determine whether this culture system could be used to measure knockdown of dSLs was not conducted under optimal conditions. The wild type neurons were cultured for only seven days, while the transgenic neurons were cultured for eleven, due to timing of working with a collaborator. Neurons are non-dividing but highly active cells, and these cells were just being established in culture over about a weeks' time. Thus it is not unexpected that a difference in total protein and sphingolipid content would exist, but it is surprising that such a large difference exists in cultures that have a difference in culture length of only four days. The health of the cultures may also impact these values, so theoretically a less robust wild type culture could result in lower values. Additionally, it may take time for

dSLs to accumulate in these neuronal preparations, and we do not know for certain if dSL levels rise rapidly after day seven. Thus based on this experiment, we cannot conclusively state that this assay distinguishes between wild type and transgenic cultures or that it can be used for examining knockdown of dSLs. However, since doxSO and doxSA are abundant in transgenic cultures and undetectable in wild type cultures, it is likely that this assay is able to distinguish between the two culture types despite sub-optimal assay design.

Another potential issue is that the culture conditions used do not allow for accurate quantitation of dSLs and so even when knockdown occurs, it cannot accurately be detected. To address this issue, we examined the d7SO-normalized values of doxSA and doxSO at two different cell numbers (one is double the other) in transgenic cultures. For appropriate assay linearity, we would expect a two fold increase in doxSA and doxSO for a two fold increase in total protein. We found that both doxSO and doxSA did not quite fit these parameters, and additionally that the species exhibited high variability, with doxSO demonstrating marked variability at the lower cell number.

These two issues indirectly impact the ability to detect knockdown of dSLs, but there were also some concerns directly impacting determination of knockdown of dSLs as well. The main concern is that the total protein concentrations of samples, though consistent within each experiment, were highly variable between experiments. This could indicate that the health of the neuronal cultures may have been different between

different preparations. Since there are varying proportions of the transgenic neurons, this variability is not entirely unexpected. In the future, cell viability should be monitored in conjunction with silencing.

For these reasons, even though a reduction in dSLs was not observed, it may be that knockdown is occurring but assay conditions are prohibiting detection of the knockdown. It is possible, however, that our lead hamster-targeting compounds do not silence dSL production, or that downregulation of LCB1 protein results in no reduction or very slow reduction of dSLs that is not able to be measured in the timecourse evaluated. The turnover rate of dSLs has not been studied systematically but is thought to be slow, as clinically dSLs accumulate in tissues and sera of affected individuals (Penno, Reilly et al. 2010). dSLs are thought to form lipid droplets in macrophages (Eichler, Hornemann et al. 2009). The low rate of turnover and accumulation are surmised to occur because dSLs lack an oxygen atom at the C1 carbon, essentially rendering the molecules resistant to further reactions (Eichler, Hornemann et al. 2009). However, evidence from serine supplementation experiments supports the notion that treatment of HSAN1 through downregulation of hamster mRNA, and thus dSLs, may result in reversal of symptoms. Serine is the normal substrate for wild type SPT and in the disease state, mutant SPT accepts serine, alanine, and glycine as substrates (Eichler, Hornemann et al. 2009). While mutant SPT is activated more often to form products when it uses alanine and glycine as substrates (Gable, Gupta et al. 2010), serine supplementation in mice and humans can overcome this competition for SPT and reduce dSL formation (Garofalo,

Penno et al. 2011). Furthermore, dietary supplementation with oral L-serine reduces dSLs and alleviates symptoms in mice and humans (Garofalo, Penno et al. 2011) C133W mice fed a 10% L-serine–enriched diet demonstrated a 5-fold decrease of doxSA and a 10-fold decrease of doxSO and reached WT dSL levels in 2–4 days (Garofalo, Penno et al. 2011). Similarly, C133Y patients dosed with 400 mg/kg/d of L-serine experienced 4-fold reduction in dSL levels within a month, reaching lowest levels after six weeks and persisting at low levels for the remainder of the ten-week study (Garofalo, Penno et al. 2011). One way of measuring turnover in our system is by temporarily blocking production of dSLs and examining rate of reduction of dSLs. dSL production could be blocked by an oligonucleotide therapeutic such as those developed here or a small molecule inhibitor of SPT.

Conclusions

We have developed and conducted initial studies laying the basis for further in vivo characterization of compounds selectively targeting SPTLC1. Based on our findings, hsiRNA-1138, ASO_414, and ASO_489 show the potential to modulate HSAN1 symptoms in transgenic animals. This study also provides evidence for primary cortical neuron culture as an appropriate in vitro model for assessing potential HSAN1 therapeutics after further optimization of cultures for dSL detection. These cultures will allow for evaluation of knockdown of mRNA, protein, and dSLs.

Importantly, hsiRNA_1138 and ASO_414 are candidates for clinical development, as they target human SPTLC1 in addition to hamster SPTLC1. There are several challenges that stand in the way of the development of these powerful oligonucleotide therapeutics for the treatment of HSAN1. There is much that is not yet known about the natural history of HSAN1. We do not know the extent of downregulation of SPTLC1 mRNA, and thus protein and dSLs that is needed to ameliorate the HSAN1 phenotype. We do know that mice heterozygous for deletion of SPTLC1 show no phenotype (Gable, Gupta et al. 2010), but homozygous knockouts display embryonic lethality (Hojjati, Li et al. 2005). There are no known C133W conditional knockout mice to assess whether SPTLC1 is only necessary during development or whether a low level of SPTLC1 is required even in adulthood of these animals. In any case, we need to determine the optimal level of silencing that alleviates symptoms but does not have negative effects due to lack of gene expression. Our protein knockdown findings support the notion that mutant LCB1 protein is relatively unstable, which could complicate development of a therapeutic strategy.

While there may be many complicating factors involved in the development and treatment of HSAN1 that are even yet to be discovered, further study of this disease is an important endeavor. There are many parallels between patients with HSAN1 and patients with Diabetes Mellitus, such as the buildup of toxic dSL species (Dohrn, Othman et al. 2015, Othman, Saely et al. 2015) in sera and tissues and the development of progressive

stocking-glove neuropathies affecting distal limbs. Investigation into reducing dSLs may benefit the myriad DM patients suffering from intractable diabetic neuropathy.

Next steps toward clinical development of these reagents involve optimizing primary neuron culture conditions to robustly quantitate dSL levels and investigating whether treatment with these reagents reduces dSL levels. Reduction of dSLs would indicate the ability of these reagents to modify a biochemical phenotypic trait of HSAN1. In vivo testing also needs to be conducted. First, biodistribution to the target tissue, DRG, and cell type, large sensory neurons, should be demonstrated. Then, confirmation of silencing efficacy in DRG, as well as pharmacokinetic and pharmacodynamic experimentation especially the investigation of duration of silencing should be undertaken. We know that long-term silencing of genes in other tissues, such as brain, with similar reagents is possible. Exploration of silencing of mutant hamster SPTLC1 vs silencing of wild type mouse SPTLC1 can elucidate the degree to which mutant SPTLC1 or both mutant and WT SPTLC1 can be silenced without adverse effects.

Appendix

Introduction:

HSAN1 affects the dorsal root ganglia (DRG) of patients (McCampbell, Truong et al. 2005). This results in loss of DRG cell bodies and denervation, as well as development of an axonal neuropathy leading to stocking-glove loss of pain and temperature sensation (Garofalo, Penno et al. 2011). We previously showed that our reagents are able to silence hamster and/or mouse SPTLC1 in in vitro systems such as the CHO-K1 cell line, mouse primary cortical neuron cultures, as well as transgenic mouse primary cortical neurons cultures derived from C133W mice (Karnam 2018). The next step in the pipeline towards clinical drug development is ascertaining the ability to target the appropriate tissue type as well as the ability to silence the gene of interest in the tissue type of interest.

HSAN1 affects the sensory neurons of the DRG and primarily involves the lower limbs (Eichler, Hornemann et al. 2009). Several subpopulations of sensory neurons exist (McCampbell, Truong et al. 2005). Within these, the small sensory neurons that are TrkA positive and those that are IB4 positive join Aδ and C fibers, which govern pain and temperature sensation (McCampbell, Truong et al. 2005). Thus this is our primary therapeutic target. Mice have 31 pairs of DRG, situated along the spinal cord, housed by the spinal column (Sleigh, Weir et al. 2016). This anatomy facilitates drug delivery to the DRG by intrathecal injection. Chemical modifications of oligonucleotide-based therapeutics are known to determine tissue specificity (Hassler, Turanov et al. 2018).

Thus we set out to determine and characterize the ability of various chemically modified oligonucleotide scaffolds to penetrate the DRG.

Methods:

WT mice were injected by lumbar intrathecal injection with varying doses of CY3-conjugated oligonucleotide scaffolds dissolved in PBS (Fig. A1). After a specified time, animals were euthanized by isoflurane overdose and transcardially perfused with PBS. Spinal columns were dissected out and either immediately post-fixed in 4% PFA or 10% formalin for 24 hours, or DRG and sometimes spinal cord were dissected out and post-fixed before being stored in PBS. Brains and livers of treated animals were also processed in some experiments. DRGs and other organs were processed, sectioned, mounted, and DAPI stained using standard protocols for histological imaging. CY3 (excitation filter 546 nm, emission filter 590 nm) and DAPI (excitation filter 350 nm, emission filter 460 nm) were imaged using a Leica DM5500 fluorescent microscope. Based on imaging, several parameters were investigated. Degree of variability refers to how variable uptake is among DRGs within the same animal. Gradient of localization from site of injection was examined in some experiments as well. In these experiments, DRGs from along the length of the spinal cord were collected and divided into three groups, close to the site of injection (lumbar region), far from the site of injection (cervical region), and mid-range (thoracic region). The degree of localization of oligonucleotide scaffolds in these various groups was compared across groups. Uptake

by sensory neurons, satellite cells or other cells, and nerve fibers was also assessed by inspection. Large sensory neurons are easily identified by their distinctly large cell bodies and nuclei, while satellite cells are smaller, with denser nuclei (Fig. A2).

A Scaffolds

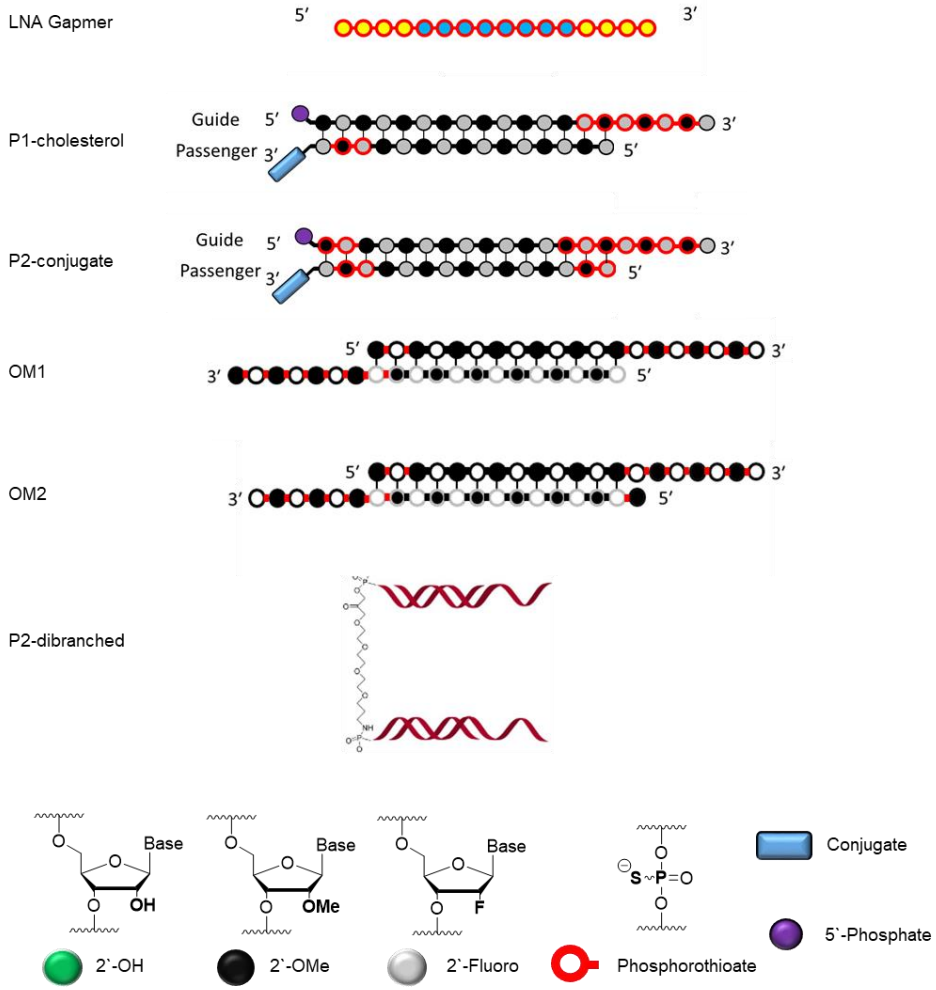

B Conjugates

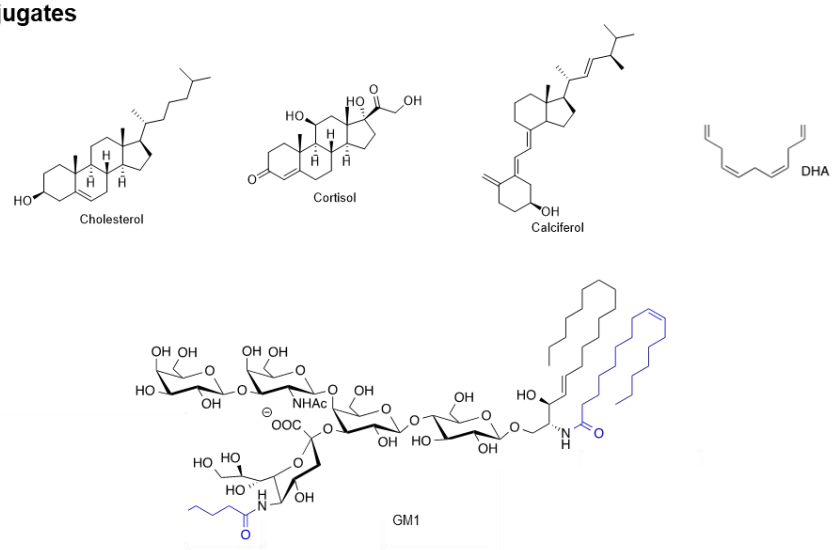

Figure A1. Structures of hsiRNA scaffolds and conjugates used in biodistribution studies

A. Various hsiRNA scaffolds were tagged with Cy3 or FYE (not shown). The P1 and P2 scaffolds were conjugated to either cholesterol (P1) or one of several hydrophobic conjugates shown in **B** (P2). The P2 dibranched structure shows two P2-Cy3 labelled hsiRNAs conjugated by tetraethylene glycol.

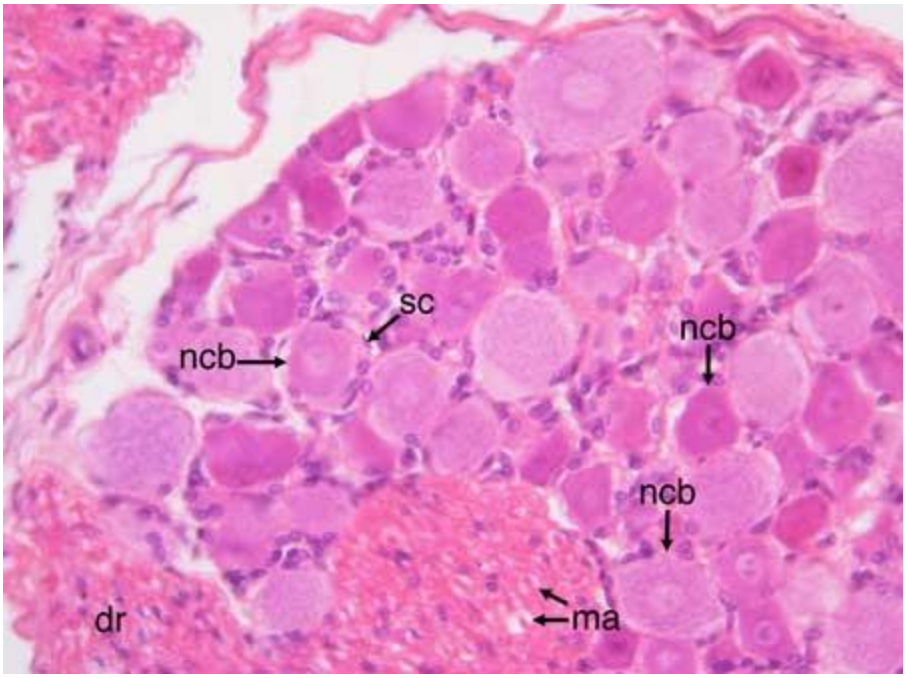

Figure A2. Dorsal Root Ganglion cellular structure
Hematoxylin-Eosin stained cross section of dorsal root ganglion shows the neuron cell bodies (ncb), satellite cells (sc), myelinated axons (ma), and dorsal root (dr). Localization experiments were performed by intrathecal injection of CY-3 labelled chemically modified oligonucleotide scaffolds, tissue processing and fluorescent microscopy of DRG. Localization to DRG tissue and to cell types was examined.

Results:

Results of the biodistribution studies are summarized in Table A1. Notably, there is marked variation in almost every parameter for most compounds tested. We are able to draw a few broad generalizations, however. For example, the LNA Gapmer seems to target the sensory neurons, as indicated by ++/+++ values in all the experiments involving this compound. In contrast, P1-cholesterol hsiRNA appears to be taken up by satellite cells and nerve fibers. P2-cholesterol hsiRNA appears to show an even greater predilection for nerve fibers, with all values ++/+++ for all experiments using this compound. P2-DHA hsiRNA demonstrates marked accumulation in satellite cells. The P2-cholecalciferol compound and the P2-dibranched compound distribute to sensory neurons, but at a lower level, ++ as compared to other compounds. OM1 and OM2 compounds appear to have promise for targeting sensory neurons as well as satellite cells.

Table A1. Results of Biodistribution Experiments

Compound	Experi-ment ID	Dose (nmol)	Time (hours)	Degree of Variability	Gradient from Site of Injection	Sensory Neuron Distribution	Satellite Cell Distribution	Nerve Fiber Distribution
LNA GapmeR	150304	6	24	Low	N/A	++	++	+++
	150307	6	24	High	-	+++	-	++
	160301	6	24	High	+++	++	++	+
P1-chol hsiRNA	150304	6	24	Low	N/A	+	+++	++
	150307	6	24	High	-	+	+	+++
	150401	6	24	0	N/A	+	++	-
	150503	6	24	Medium	+++	++	++	++
P2-chol hsiRNA	150304	6	24	High	+++	+	-	+++
	150307	6	24	0	-	++	+	++
	150503	6	24	Medium	++	+++	+	+++
	151116	6	24	N/A	N/A	+	-	++
	160301	6	24	High	+++	++	++	+++
P2-GM1 hsiRNA	150415	10	48	N/A	N/A	-	-	-
P2-DHA hsiRNA	150401	6	24	N/A	-	++	+++	+
	150415	10	48	N/A	N/A	+	+++	-
	150503	6	24	0	-	++	+++	++
P2-cholecalciferol hsiRNA	150415	10	48	N/A	N/A	++	+	-
	150604	6	24	High	++	++	-	+
	151116	6	24	High	N/A	+	-	-
P2-cortisol hsiRNA	150415	10	48	N/A	N/A	+	+++	-
OM1-hsiRNA	150618	10	48	0	N/A	+++	+++	+
OM2-hsiRNA	150618	10	48	0	N/A	++	+++	-
P2-Di branched hsiRNA	151116	6	24	N/A	N/A	++	-	++
	160301	6	24	Low	+	+	+++	-

Table A1.

Degree of Variability – how variable is uptake among DRGs within the same animal?

0 – no variability appreciable

Low – low degree of variability among DRGs examined

Medium – there is some difference among DRGs as to how much oligonucleotide they take up

High – some DRG take up the oligonucleotide to a high degree, whereas others do not take up the oligonucleotide at all

N/A – Not Assessed

Gradient from Site of Distribution – how far from the site of injection did the oligonucleotide distribute?

- – no gradient appreciable

+ – not much change in distribution across the length of the spinal cord

++ – moderate change in distribution across the length of the spinal cord

+++ – high degree of change in distribution across the length of the spinal cord

N/A – Not Assessed (i.e. only DRGs from the same general area with respect to the spinal cord were examined, whether lumbar, thoracic, or cervical)

Sensory Neuron/Satellite Cell/Nerve Fiber Distribution – how intense is the CY3 localization?

- – No visible distribution

+ – low level of distribution, dim

++ – moderate level of distribution

+++ – high level of distribution, very bright

Discussion:

The high level of variability in almost all parameters evaluated obscures definitive interpretation of the data. This is exacerbated by the fact that some compounds only had one or two experiments investigating their biodistribution. Furthermore, it is difficult to draw conclusions because the experiments were not uniform, and variables such as dose as well as timecourse were altered in some cases and so results are not directly comparable. However, even among the experiments with the standardized variables of 6 nanomole dose and 24 hour timepoint, there still is a lot of variability. A contributing factor is that some experiments had only one animal in the experiment per group, but this is less of a concern since in most cases several DRGs were assessed per animal, or in many cases, per spinal cord region.

Perhaps the most defining issue is that after these DRGs were dissected out, they were processed by the histology core. Thus these samples may have been exposed to light for varying lengths of time, which may impact the variability observed between experiments as well as reduce the amount of oligonucleotide observed in tissue. Localization of other, similar chemical scaffolds to DRG has been investigated in the Khvorova lab by removing, demineralizing, and sectioning the whole spinal column. These investigations show robust and more consistent delivery of these oligonucleotides to the DRG (data not shown). Thus these oligonucleotides may represent better chemical configuration to target the DRG, or the tissue processing method is one which better preserves signal from the CY3-labelled compounds. DRG biodistribution of a single compound should be

assessed, comparing the two tissue processing methods, to determine whether the processing method is a factor affecting ability to detect localization to DRG.

Another potential factor is the fact that in many experiments, a gradient of cellular uptake was observed, whereby there was a greater degree of uptake of oligonucleotides closer to the injection site as compared to further away from the injection site. This could be the result of high viscosity of the hydrophobic oligonucleotides, which may not migrate or disperse efficiently. In the future, this issue could be addressed by diluting the compounds to a lower concentration and injecting a larger bolus or pump infusion of the compounds. Additionally, more animals per group should be used in each study. Another factor that could be contributing to variability is the fact that different sequences were used for localization experiments. It is known that chemical modifications contribute to tissue specificity (Hassler, Turanov et al. 2018), and previous experimentation from the Khvorova lab indicates that sequence differences do not contribute to localization patterns. Once these factors have been optimized, DRG localization should be examined in closer detail with markers identifying and distinguishing different populations of cells.

References:

(2018). "Alnylam Presents New Clinical Results from the APOLLO Phase 3 Study of Patisiran at the 16th International Symposium on Amyloidosis." from http://investors.alnylam.com/news-releases/news-release-details/alnylam-presents-new-clinical-results-apollo-phase-3-study.

Alterman, J. F., A. H. Coles, L. M. Hall, N. Aronin, A. Khvorova and M. C. Didiot (2017). "A High-throughput Assay for mRNA Silencing in Primary Cortical Neurons in vitro with Oligonucleotide Therapeutics." Bio Protoc **7**(16).

Alterman, J. F., L. M. Hall, A. H. Coles, M. R. Hassler, M. C. Didiot, K. Chase, J. Abraham, E. Sottosanti, E. Johnson, E. Sapp, M. F. Osborn, M. Difiglia, N. Aronin and A. Khvorova (2015). "Hydrophobically Modified siRNAs Silence Huntingtin mRNA in Primary Neurons and Mouse Brain." Mol Ther Nucleic Acids **4**: e266.

Auer-Grumbach, M. (2008). "Hereditary sensory neuropathy type I." Orphanet J Rare Dis **3**: 7.

Bejaoui, K., D. McKenna-Yasek, B. A. Hosler, E. Burns-Deater, L. M. Deater, G. O'Neill, J. L. Haines and R. H. Brown, Jr. (1999). "Confirmation of linkage of type 1 hereditary sensory neuropathy to human chromosome 9q22." Neurology **52**(3): 510-515.

Bejaoui, K., C. Wu, M. D. Scheffler, G. Haan, P. Ashby, L. Wu, P. de Jong and R. H. Brown, Jr. (2001). "SPTLC1 is mutated in hereditary sensory neuropathy, type 1." Nat Genet **27**(3): 261-262.

Birmingham, A., E. Anderson, K. Sullivan, A. Reynolds, Q. Boese, D. Leake, J. Karpilow and A. Khvorova (2007). "A protocol for designing siRNAs with high functionality and specificity." Nat Protoc **2**(9): 2068-2078.

Bode, H., F. Bourquin, S. Suriyanarayanan, Y. Wei, I. Alecu, A. Othman, A. Von Eckardstein and T. Hornemann (2016). "HSAN1 mutations in serine palmitoyltransferase reveal a close structure-function-phenotype relationship." Hum Mol Genet **25**(5): 853-865.

Dawkins, J. L., D. J. Hulme, S. B. Brahmbhatt, M. Auer-Grumbach and G. A. Nicholson (2001). "Mutations in SPTLC1, encoding serine palmitoyltransferase, long chain base subunit-1, cause hereditary sensory neuropathy type I." Nat Genet **27**(3): 309-312.

Dohrn, M. F., A. Othman, S. K. Hirshman, H. Bode, I. Alecu, E. Fahndrich, W. Karges, J. Weis, J. B. Schulz, T. Hornemann and K. G. Claeys (2015). "Elevation of plasma 1-deoxy-sphingolipids in type 2 diabetes mellitus: a susceptibility to neuropathy?" Eur J Neurol **22**(5): 806-814, e855.

Eichler, F. (2017). "L-Serine Supplementation in Hereditary Sensory Neuropathy Type 1." September 3rd, 2018, from https://clinicaltrials.gov/ct2/show/NCT01733407.

Eichler, F. (2018) "Hereditary sensory and autonomic neuropathies."

Eichler, F. S., T. Hornemann, A. McCampbell, D. Kuljis, A. Penno, D. Vardeh, E. Tamrazian, K. Garofalo, H. J. Lee, L. Kini, M. Selig, M. Frosch, K. Gable, A. von Eckardstein, C. J. Woolf, G. Guan, J. M. Harmon, T. M. Dunn and R. H. Brown, Jr. (2009). "Overexpression of the wild-type SPT1 subunit lowers desoxysphingolipid levels and rescues the phenotype of HSAN1." J Neurosci **29**(46): 14646-14651.

Gable, K., S. D. Gupta, G. Han, S. Niranjanakumari, J. M. Harmon and T. M. Dunn (2010). "A disease-causing mutation in the active site of serine palmitoyltransferase causes catalytic promiscuity." J Biol Chem **285**(30): 22846-22852.

Garofalo, K., A. Penno, B. P. Schmidt, H. J. Lee, M. P. Frosch, A. von Eckardstein, R. H. Brown, T. Hornemann and F. S. Eichler (2011). "Oral L-serine supplementation reduces production of neurotoxic deoxysphingolipids in mice and humans with hereditary sensory autonomic neuropathy type 1." J Clin Invest **121**(12): 4735-4745.

Hanada, K. (2003). "Serine palmitoyltransferase, a key enzyme of sphingolipid metabolism." Biochim Biophys Acta **1632**(1-3): 16-30.

Hassler, M. R., A. A. Turanov, J. F. Alterman, R. A. Haraszti, A. H. Coles, M. F. Osborn, D. Echeverria, M. Nikan, W. E. Salomon, L. Roux, B. Godinho, S. M. Davis, D. V. Morrissey, P. D. Zamore, S. A. Karumanchi, M. J. Moore, N. Aronin and A. Khvorova (2018). "Comparison of partially and fully chemically-modified siRNA in conjugate-mediated delivery in vivo." Nucleic Acids Res **46**(5): 2185-2196.

Hojjati, M. R., Z. Li and X. C. Jiang (2005). "Serine palmitoyl-CoA transferase (SPT) deficiency and sphingolipid levels in mice." Biochim Biophys Acta **1737**(1): 44-51.

Karnam, H. (2018). Chemically Modified Oligonucleotides Silence Mutant SPTLC1 in an in vitro Model of HSAN1 University of Massachusetts Medical School.

Khvorova, A. and J. K. Watts (2017). "The chemical evolution of oligonucleotide therapies of clinical utility." Nat Biotechnol **35**(3): 238-248.

McCampbell, A., D. Truong, D. C. Broom, A. Allchorne, K. Gable, R. G. Cutler, M. P. Mattson, C. J. Woolf, M. P. Frosch, J. M. Harmon, T. M. Dunn and R. H. Brown, Jr. (2005). "Mutant SPTLC1 dominantly inhibits serine palmitoyltransferase activity in vivo and confers an age-dependent neuropathy." Hum Mol Genet **14**(22): 3507-3521.

Nicholson, G. A. (2006). "The dominantly inherited motor and sensory neuropathies: clinical and molecular advances." Muscle Nerve **33**(5): 589-597.

Nicholson, G. A., J. L. Dawkins, I. P. Blair, M. Auer-Grumbach, S. B. Brahmbhatt and D. J. Hulme (2001). "Hereditary sensory neuropathy type I: haplotype analysis shows founders in southern England and Europe." Am J Hum Genet **69**(3): 655-659.

Osborn, M. F., A. H. Coles, D. Golebiowski, D. Echeverria, M. P. Moazami, J. K. Watts, M. Sena-Esteves and A. Khvorova (2018). "Efficient Gene Silencing in Brain Tumors with Hydrophobically Modified siRNAs." Mol Cancer Ther **17**(6): 1251-1258.

Othman, A., C. H. Saely, A. Muendlein, A. Vonbank, H. Drexel, A. von Eckardstein and T. Hornemann (2015). "Plasma 1-deoxysphingolipids are predictive biomarkers for type 2 diabetes mellitus." BMJ Open Diabetes Res Care **3**(1): e000073.

Penno, A., M. M. Reilly, H. Houlden, M. Laura, K. Rentsch, V. Niederkofler, E. T. Stoeckli, G. Nicholson, F. Eichler, R. H. Brown, Jr., A. von Eckardstein and T. Hornemann (2010). "Hereditary sensory neuropathy type 1 is caused by the accumulation of two neurotoxic sphingolipids." J Biol Chem **285**(15): 11178-11187.

Shen, X. and D. R. Corey (2017). "Chemistry, mechanism and clinical status of antisense oligonucleotides and duplex RNAs." Nucleic Acids Res.

Sleigh, J. N., G. A. Weir and G. Schiavo (2016). "A simple, step-by-step dissection protocol for the rapid isolation of mouse dorsal root ganglia." BMC Res Notes **9**: 82.

Suh, B. C., Y. B. Hong, K. Nakhro, S. H. Nam, K. W. Chung and B. O. Choi (2014). "Early-onset severe hereditary sensory and autonomic neuropathy type 1 with S331F SPTLC1 mutation." Mol Med Rep **9**(2): 481-486.

Watts, J. K. and D. R. Corey (2012). "Silencing disease genes in the laboratory and the clinic." J Pathol **226**(2): 365-379.

Wright, P. D., M. Huang, A. Weiss, J. Matthews, N. Wightman, M. Glicksman and R. H. Brown, Jr. (2010). "Screening for inhibitors of the SOD1 gene promoter: pyrimethamine does not reduce SOD1 levels in cell and animal models." Neurosci Lett **482**(3): 188-192.